Early childhood development of white matter fiber density and morphology

Dennis Dimond[a,b,c,d*], Christiane S. Rohr[b,c,d], Robert E. Smith[e,f], Thijs Dhollander[e,f], Ivy Cho[g], Catherine Lebel[b,c,d,h,i], Deborah Dewey[b,d,h,j,k], Alan Connelly[e,f], Signe Bray[b,c,d,h,i,l,]

[a] Department of Neuroscience, Cumming School of Medicine, University of Calgary, Calgary, AB, Canada

[b] Alberta Children's Hospital Research Institute, University of Calgary, Calgary, AB, Canada.

[c] Child and Adolescent Imaging Research Program, University of Calgary, Calgary, AB, Canada.

[d] Hotchkiss Brain Institute, University of Calgary, Calgary, AB, Canada

[e] The Florey Institute of Neuroscience and Mental Health, Melbourne, VIC, Australia

[f] The Florey Department of Neuroscience and Mental Health, The University of Melbourne, Melbourne, VIC, Australia

[g] Department of Psychological Clinical Sciences, University of Toronto, Toronto, ON, Canada

[h] Owerko Centre, University of Calgary, Calgary, AB, Canada

[i] Mathison Centre for Mental Health Research and Education, University of Calgary, Calgary, AB, Canada

[j] Department of Paediatrics, Cumming School of Medicine, University of Calgary, Calgary, AB, Canada.

[k] Department of Community Health Sciences, University of Calgary, Calgary, AB, Canada

[l] Department of Radiology, Cumming School of Medicine, University of Calgary, Calgary, AB, Canada

Correspondence: * indicates corresponding author

Dennis Dimond; dennis.dimond@ucalgary.ca ; 1-403-955-5704; Alberta Children's Hospital, 28 Oki Drive NW, Calgary, Alberta, Canada, T3B 6A8.

Running title: Fiber density and cross-section maturation during early childhood

ABSTRACT

Early childhood is an important period for cognitive and brain development, though white matter changes specific to this period remain understudied. Here we utilize a novel analytic approach to quantify and track longitudinal changes in white matter micro- and macro-structure, calculated from individually oriented fiber-bundle populations, termed “fixels”. Fixel-based analysis and mixed-effects models were used to assess tract-wise changes in fiber density and bundle morphology in 73 girls scanned at baseline (ages 4.09-7.02, mean=5.47, SD=0.81), 6-month (N=7), and one-year follow-up (N=42). We also assessed changes in fractional anisotropy (FA) and mean diffusivity (MD). Maturational increases in fixel-metrics were seen in most major white matter tracts, with the most rapid increases in the corticospinal tract and slowest or non-significant increases in the genu of the corpus callosum and uncinate fasciculus. As expected, we observed developmental increases in FA and decreases in MD, though percentage changes were smaller than fixel-metrics. The majority of tracts showed more substantial morphological than microstructural changes. These findings highlight early childhood as a period of dynamic white matter maturation, characterized by large increases in macroscopic fiber bundle size, mild changes in axonal density, and parallel, albeit less substantial, changes in diffusion tensor metrics.

Key words: Early childhood; Fiber bundle morphology; Fiber density; Fixel-based analysis; White matter

Early childhood is a period of rapid cognitive and behavioral maturation, with profound changes in attention, working memory, reading, math, and self-regulatory abilities (Ferretti et al. 2008; Burnett Heyes et al. 2012; Breckenridge et al. 2013; Montroy et al. 2016; Garon-Carrier et al. 2018). Maturation of these essential cognitive-behavioral skills is believed to be related to white matter growth in the brain (Qiu et al. 2008; Van Eimeren et al. 2008; Klarborg et al. 2013; Jolles et al. 2016; Bathelt et al. 2018), though developmental trajectories of white matter maturation and the biological underpinnings of these changes remain poorly understood. The reason for this is two-fold. Firstly, while white matter development throughout the lifespan has been well characterized (Westlye et al. 2010; Lebel et al. 2012; Yeatman et al. 2014), few studies have focused on white matter changes during early childhood. Secondly, most studies make use of the diffusion tensor model (subsequently referred to simply as diffusion tensor imaging or "DTI"), which provides only limited insight into the biological changes underlying white matter growth. This limitation is due to the unreliability of DTI metrics in regions of crossing/kissing fibers (Jeurissen et al. 2013) and the fact that such metrics are potentially sensitive to a range of microstructural features. Age-related changes in fractional anisotropy (FA) and mean diffusivity (MD) from birth to adulthood have been suggested to potentially reflect developmental increases in axonal packing, myelination, or so-called white matter "integrity" (Lebel and Deoni 2018), but it is not possible to infer information related to specific tracts or to be clear which biological features are changing using these metrics. Studies utilizing higher-order diffusion models are necessary to provide a more specific description of changes in white matter structural properties during early childhood.

Advanced diffusion imaging techniques, which provide metrics with greater structural specificity, are increasingly being applied to investigate white matter development. One such technique is fixel-based analysis (FBA; (Raffelt, Tournier, et al. 2017)), which is a novel approach to quantify and analyze white matter micro- and macro-structure within "fixels" (specific fiber-bundle populations within a voxel (Raffelt et al. 2015)). FBA can be utilized in combination with constrained spherical

deconvolution (CSD) techniques (Tournier et al. 2007; Jeurissen et al. 2014; Dhollander and Connelly 2016) to delineate multiple fiber bundle populations within a voxel, making it possible to calculate and assess fixel-wise metrics sensitive to axonal density/packing ("Fiber Density (FD)"), fiber bundle cross-sectional size ("Fiber Cross-section (FC)"), and a combined measure encompassing both micro- and macrostructure ("Fiber Density and Cross-section (FDC)") [Raffelt et al., 2017a]. These metrics are arguably of greater specificity and interpretability than voxel-wise DTI metrics like FA and MD (Raffelt, Tournier, et al. 2017).

Studies utilizing FBA in a neurodevelopmental context suggest white matter development from late childhood to early adulthood may be driven by increases in both axonal packing/density and fiber bundle size (Genc, Seal, et al. 2017; Genc, Malpas, et al. 2018; Genc, Smith, et al. 2018; Genc et al. 2019). Age-related increases in axonal packing/density from late childhood to adulthood have also been suggested by studies utilizing an alternative diffusion model, "neurite orientation and dispersion density imaging (NODDI)" (Chang et al. 2015; Genc, Malpas, et al. 2017; Mah et al. 2017); these changes have been shown to occur alongside increasing FA and decreasing MD during late childhood to adulthood and correlate more strongly with age than DTI metrics (Genc, Malpas, et al. 2017; Mah et al. 2017). Taken together, these findings suggest that increasing axonal density/packing and fiber bundle size underlie the DTI changes observed in late-childhood to adulthood, though whether this is the case in early childhood remains unclear.

Brain development is notably heterochronous, and spatial trends in white matter development during early childhood remain relatively unclear. Lifetime changes in FA and MD have been shown to occur across major white matter tracts in a posterior-to-anterior fashion, with earliest maturation of projection and commissural fibers, followed by association fibers, and then frontal-temporal fibers, which mature into adulthood (Lebel et al. 2012). A recent large sample study in children ages 2-8 years provides evidence in support of this pattern, showing that changes in diffusion tensor metrics (FA and

MD) across early childhood are more rapid in posterior regions as compared to frontal-temporal tracts (Reynolds et al. 2019). This spatial trend is also supported by FBA (Genc, Smith, et al. 2018) and NODDI (Mah et al. 2017) studies showing that axonal density/packing changes during late childhood are greatest in the forceps major, a posterior commissural fiber. These findings suggest that developmental changes in axonal density may follow a similar spatial pattern to changes observed in DTI metrics.

The aim of the current study was to characterize longitudinal changes in axonal packing/density and fiber bundle size of major white matter tracts during early childhood. To do this, we utilized 3-tissue CSD (Dhollander and Connelly 2016) in conjunction with FBA (Raffelt, Tournier, et al. 2017) to assess tract-wise changes in FBA metrics (FD, FC and FDC) in typically developing girls aged 4-8 years, scanned at baseline, 6-month and 12-month follow-up. To compare our findings to more commonly used DTI metrics, we also assessed changes in FA and MD. Considering previous literature suggestive of widespread developmental increases in axonal packing and fiber bundle size from late childhood to adulthood (Chang et al. 2015; Genc, Malpas, et al. 2017, 2018; Mah et al. 2017; Genc, Smith, et al. 2018), we hypothesized that FD, FC, and FDC would all increase longitudinally throughout the whole brain (but particularly in major white matter tracts), indicative of ubiquitous axonal density and cross-sectional fiber bundle growth during early childhood. Furthermore, considering evidence for varying rates of maturation across white matter tracts (Lebel et al. 2012; Reynolds et al. 2019), we hypothesized that FD, FC and FDC changes would be most rapid in commissural and projection fibers, and slowest in frontal-temporal tracts.

MATERIALS AND METHODS

Participants

Seventy-six typically developing girls were recruited from the Calgary area and underwent diffusion MRI scanning and cognitive testing at baseline (ages 4.09-7.02, mean=5.47, SD=0.81). A subset also

participated in 6-month (N=7, ages 4.61-7.01, mean=5.57, SD=0.77) and 12-month (N=43, ages 5.13-7.89, mean=6.43, SD=0.74) follow-up scans. Four data sets, 3 of which belonged to participants with only one time-point, were excluded from the study due to poor data quality (described in more detail below). The final sample therefore consisted of 122 total scans collected from 73 participants at baseline (N=73), 6-month follow-up (N=7), and 12-month follow-up (N=42). The study was approved by the Conjoint Health and Research Ethics Board at the University of Calgary. Informed consent was obtained from the parents and informed assent from the participants.

Data acquisition

Data were collected at the Alberta Children's Hospital and included diffusion and structural (T1-weighted) MR images, as well as handedness. MRI data were acquired on a 3T GE MR750w (Waukesha, WI) scanner using a 32-channel head coil. Diffusion-weighted images (DWIs) were acquired using a 2D spin echo EPI sequence (b=2000s/mm^2, 45 diffusion-weighted directions, 3 non-DWI (*b*=0) images, 2.5mm^3 isotropic voxels, 45 slices, 23x23cm FOV, TE=86.2ms, TR=10s). Structural images were obtained using a T1-weighted 3D BRAVO sequence (0.8mm^3 isotropic voxels, 24x24cm FOV, TI=600ms, FA=10°).

Structural image processing

Structural T1-weighted images were utilized to calculate intra-cranial volume (ICV) for use as a nuisance covariate in statistical analysis. It is generally recommended that ICV be included as a covariate in FBA to account for relative differences in head size, which may vary with age and thus potentially influence morphological fixel-based white matter metrics (fiber cross-section (FC) in particular). T1-weighted images were bias field corrected (Tustison et al. 2010), and ICV estimated using the Computational Anatomy Toolbox (CAT; http://www.neuro.uni-jena.de/cat/) in SPM 12 (https://www.fil.ion.ucl.ac.uk/spm/software/spm12/).

DWI preprocessing and motion assessment

To mitigate effects of head motion, which are particularly prevalent in this age range, we utilized current state-of-the-art DWI pre-processing (Andersson and Sotiropoulos 2016) provided in *FSL* (Jenkinson et al. 2012), including replacement of slice-wise signal dropout (Andersson et al. 2016) and within-volume motion correction (Andersson et al. 2017). DWI volumes for which more than 20% of slices were classified as containing signal dropout were removed from the data, and scans for which more than 10% of volumes were removed were excluded from the study entirely (resulting in the exclusion of 4 scans from 3 participants). To quantify and control for the potential influence of head motion on outcome measures, we calculated the total number of signal dropout slices per dataset for use as a covariate in statistical analyses. Following motion correction, bias fields estimated from the mean *b*=0 images were utilized to bias field correct the DWIs (Tustison et al. 2010; Raffelt, Tournier, Rose, et al. 2012), which were subsequently upsampled to 1.25mm^3 isotropic voxels.

FBA and fixel metrics

To calculate fixel-based metrics we generally followed the *MRtrix3* (Tournier et al. 2019) FBA processing pipeline[1] (Raffelt, Tournier, et al. 2017), with the exception that instead of using the standard constrained spherical deconvolution approach (Tournier et al. 2007) estimation of white matter fiber orientation distributions (FODs) was done for each participant via "single-shell 3-tissue constrained spherical deconvolution" (SS3T-CSD) (Dhollander and Connelly 2016) using a group averaged response function for each tissue type (white matter, grey matter and CSF) (Raffelt, Tournier, Rose, et al. 2012; Dhollander et al. 2016). The remaining processing steps included: global intensity normalization of FOD images (Raffelt, Dhollander, et al. 2017); generation of a study-specific FOD template (Raffelt et al. 2011); registration of FOD images to template space (Raffelt, Tournier, Crozier, et al. 2012); segmentation of both template and per-scan FODs in template space to identify discrete fixels [Smith et

[1] https://mrtrix.readthedocs.io/en/3.0_rc2/fixel_based_analysis/mt_fibre_density_cross-section.html

al., 2013]; and identification and assignment of corresponding fixels between the scans and the template (Raffelt et al. 2015).

Following these processing steps, we calculated the three standard fixel-based metrics for FBA [Raffelt et al., 2017a]:

1) *Fiber density (FD)*: a microstructural metric that serves as a proxy for axonal density or packing;
2) *Fiber cross-section (FC)*: a macrostructural metric that approximates relative fiber bundle diameter or size;
3) *Fiber density and cross-section (FDC)*: the product of FD and FC, which encapsulates changes to both micro- and macro-structure.

Template-based tractography and tract means

A whole-brain tractogram was first generated via probabilistic tractography (Tournier et al. 2010) performed on the FOD template (Raffelt et al. 2015) using random seeding throughout the entire template, with 20 million streamlines generated (tractography parameters: step size=0.625mm, max angle between steps=22.5°, min/max fiber length=10mm/250mm, cut-off FOD amplitude=0.1). Spherical-deconvolution informed filtering of tractograms (SIFT) (Smith et al. 2013) was then used to reduce the tractogram to 2 million streamlines exhibiting reduced global reconstruction biases.

We extracted major white matter tracts of interest from this tractogram using manually-defined inclusion and exclusion ROIs (Supplementary Table 1). These tracts included: the arcuate fasciculi, cingulum bundles, corticospinal tracts, fornix bundles, inferior frontal-occipital fasciculi, inferior longitudinal fasciculi, superior longitudinal fasciculi and uncinate fasciculi, as well as the genu, body and splenium of the corpus callosum and their projections to the cortex (Figure 1).

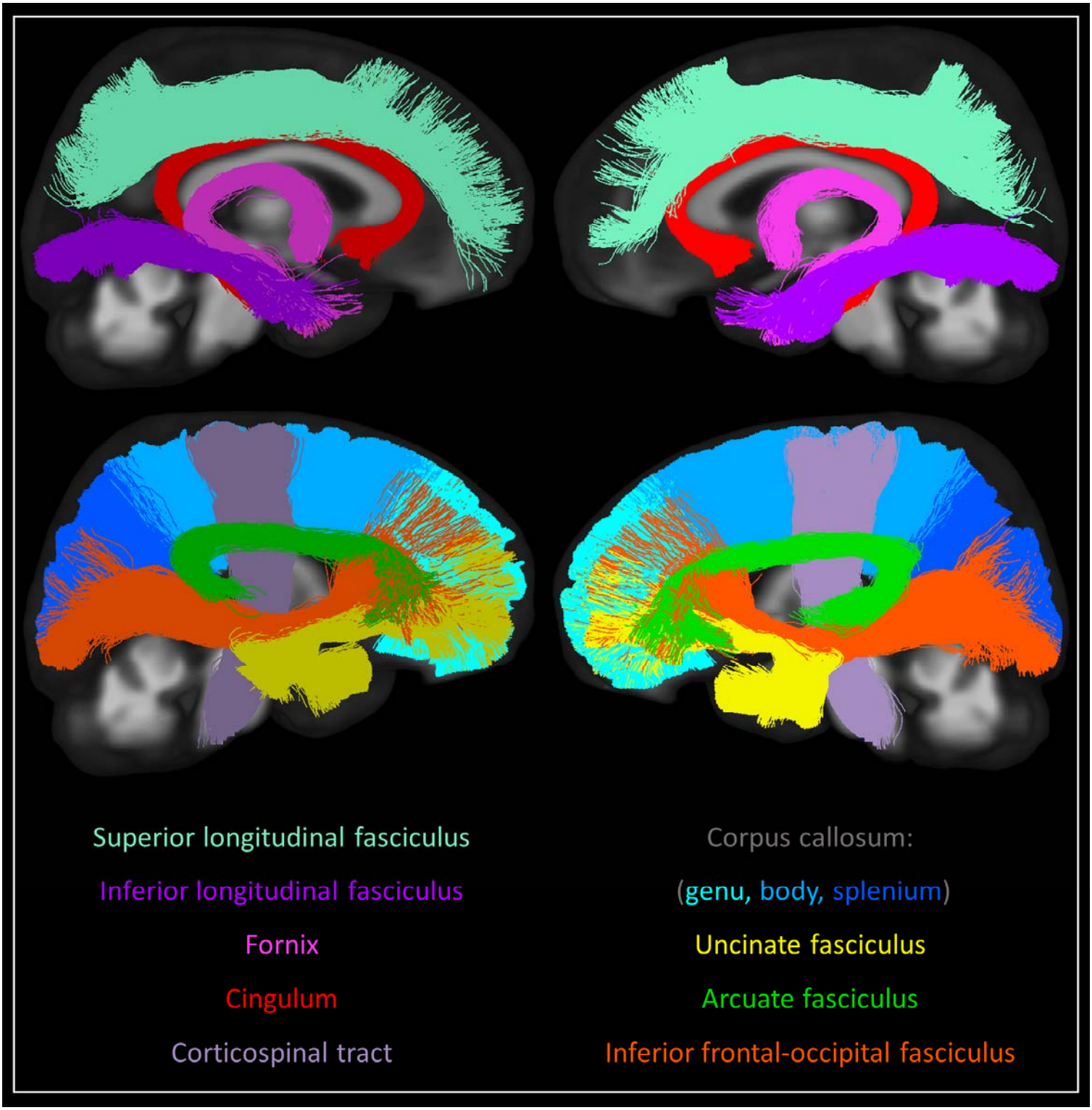

Figure 1. Tracts of interest. Bilateral white matter tracts of interest included in the study. Three-dimensional tracts are overlaid onto 2D slices of study template space and coloured according to the figure legend. Tracts are approximately split into medial (top row) and lateral (bottom row) groups for visual clarity.

These tracts were utilized to create both voxel and fixel masks. For each bundle, only fixels through which at least 5 streamlines passed, and that had a maximum template FOD amplitude of at least 0.1, were included in the fixel mask for that bundle; a corresponding voxel mask was then constructed that included all voxels containing at least one fixel within the respective mask.

For each scan, we calculated the mean FD, FC, FDC, MD and FA of each tract, by averaging values of the template-normalized metric images across voxels/fixels contained within the relevant masks (voxel masks for MD and FA; fixel masks for FD, FC and FDC). Additionally, to assess global brain changes, we generated global white matter voxel/fixel masks based on a maximum template FOD amplitude threshold of 0.1 and calculated mean values of voxel/fixel-wise metrics within these masks for each subject. This "global white matter mask" therefore included white matter voxels/fixels beyond those encompassed by the tract-wise masks.

Statistical analysis

To assess changes in tract-wise diffusion metrics with age, we utilized linear mixed effects models performed using *lme4* (Bates et al. 2017) in *R* (R Core Team 2014). For all models we included age, handedness, ICV, and total number of signal dropout slices as fixed effects, and participant-specific intercepts as a random effect. Visual inspection revealed no obvious non-linear relationships or deviations from homoscedasticity or residual normality. P-values for t-statistics were obtained using the Satterthwaite's degrees of freedom method (Hrong-Tai Fai and Cornelius 2007), as implemented in *lmerTest* (Kuznetsova et al. 2017). False discovery rate (FDR) was utilized to control for multiple comparisons within metrics, with statistical inference set at $p<0.05$. For comparison of relative growth within tracts, we calculated the percent increase in a given metric by dividing the predicted value at age 8 by the predicted value at age 4. Rates of change, predicted values at ages 4 and 8, and percent increases for each imaging metric are provided in Supplementary Tables 2-6.

Data visualization

For each imaging metric (FA, MD, FD, FC, FDC) we provide a figure with three panels: panel A shows tract-wise rates of change with confidence intervals to facilitate comparison of maturational rates across tracts; panel B shows linear developmental trajectories, to illustrate tract-wise developmental patterns and facilitate comparison of metric values; panel C shows an anatomical heat-map image of tract-wise rates of change, to illustrate spatial trends. A scatterplot of individual scan global white matter values is provided for each metric in Supplementary Figure 1. Following within-metric findings, we summarize trends in development of each tract across metrics by converting tract-wise rates of change to z-scores. For each imaging metric of interest individually, the rates of change across all regions of interest (19 tracts, as well as the global white matter mask) were converted to z-scores; thus, five z-scores were produced for each region of interest (one for each imaging metric). Here, MD z-scores were negated to facilitate comparison of across metrics, given MD has a negative relationship with age, unlike other metrics utilized in the study. The resulting z-scores are plotted alongside one another for visual comparison, and an anatomical image in which the five z-scores (one for each imaging metric) are averaged within tracts is provided to illustrate spatial trends.

RESULTS

Fiber Density (FD)

Significant increases in FD were seen bilaterally in the arcuate fasciculi, cingulum bundles, and corticospinal tracts, as well as the body and splenium of the corpus callosum, the right inferior frontal-occipital fasciculus, and the global white matter mask (Figure 2A-B). The most rapid increases were seen in the bilateral corticospinal tract and splenium of the corpus callosum; slower statistically significant increases were seen in the body of the corpus callosum and global white matter mask; changes in the genu of the corpus callosum, fornix bundles, left inferior frontal-occipital fasciculus, inferior longitudinal

fasciculus, superior longitudinal fasciculi and uncinate fasciculi were not significant. Across those tracts with statistically significant growth, FD values increased by 3.1-7.1% (Supplementary Table 2); the largest percentage increases were seen in the splenium of the corpus callosum (7.1%), the left arcuate fasciculus (6.8%), and the right cingulum (6.2%). Spatially, tracts extending into frontal cortex (i.e. the genu of the corpus callosum, inferior frontal-occipital fasciculi, and uncinate fasciculi) and temporal lobes (i.e. the inferior longitudinal fasciculi and uncinate fasciculi) showed slower and/or non-significant FD changes (Figure 2C).

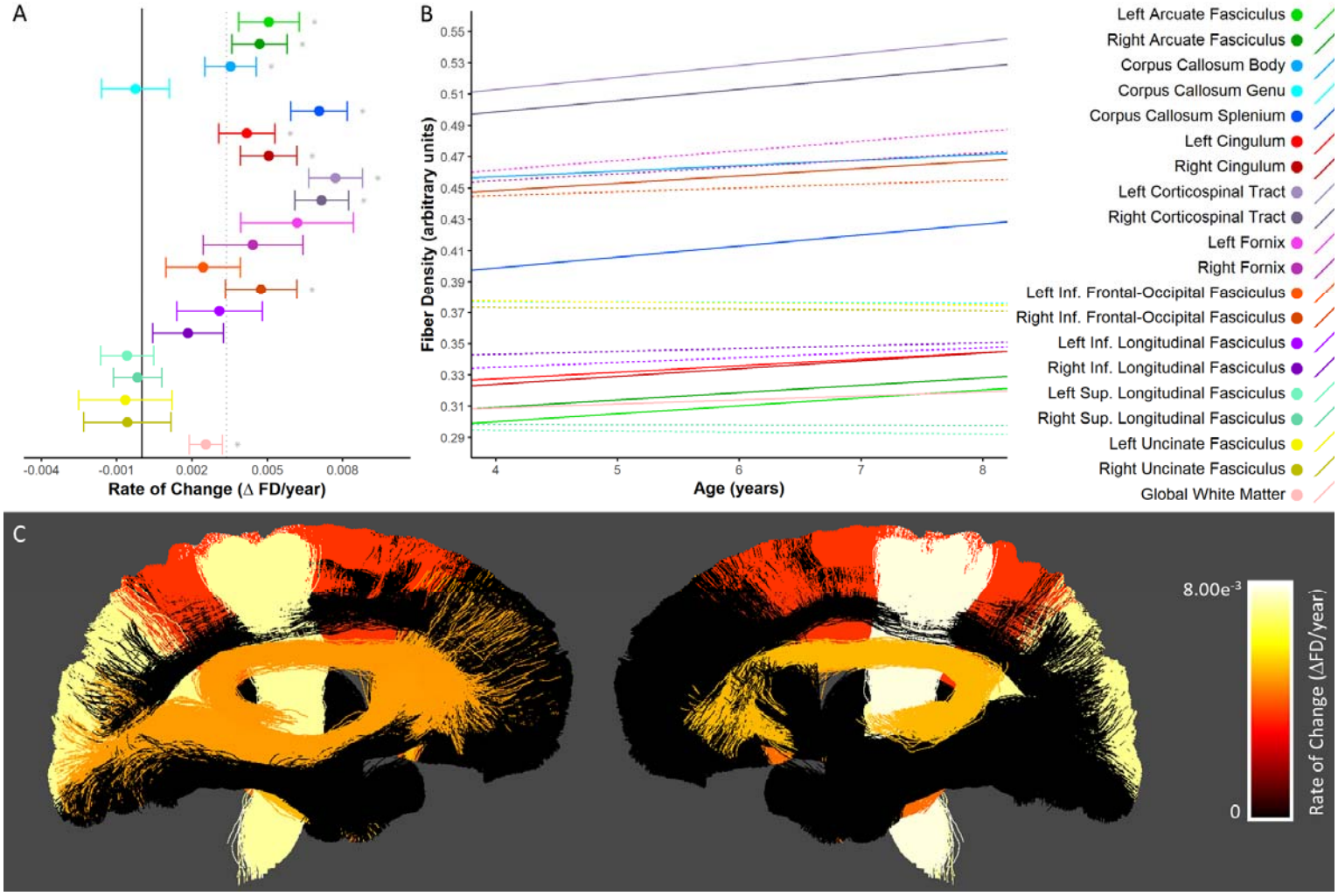

Figure 2. Developmental changes in fiber density. A) Rate of change in FD shown for each tract. * denotes tracts in which changes were statistically significant ($p<0.05$). The solid black vertical line indicates zero change, while the dotted gray vertical line indicates the mean rate of change across all tracts. B) Linear trajectories of FD growth for each tract. Solid lines indicate tracts in which there was a statistically significant relationship with age; dotted lines correspond to non-significant tracts. C) Anatomical visualization of tract-wise rates of change in FD. Streamlines corresponding to each tract are coloured according to the rate of change of FD observed in that tract. Streamlines belonging to tracts in which the rate of change was not significantly greater then zero were assigned a value of zero and appear black in the figure.

Fiber Cross-section (FC)

Significant FC increases were seen in all white matter tracts assessed here except for the genu of the corpus callosum (Figure 3A-B). Across tracts with statistically significant growth, the most rapid increases occurred in the bilateral corticospinal tract and inferior longitudinal fasciculi, while slower increases were observed in the bilateral cingulum, uncinate fasciculi, and fornix bundles. Percentage increases ranged from 3.87-13.0% (Supplementary Table 3) across tracts with statistically significant growth. Percent increases mirrored absolute rates of change, with the greatest percentage increases in the bilateral corticospinal tract and the smallest increase in the right uncinate fasciculus. Spatially, increases were more rapid in posterior brain regions, with slower maturation in tracts that connect to the frontal cortex (i.e. the uncinate fasciculi, and genu of the corpus callosum), as well as in tracts connecting deep brain structures (i.e. the cingulum and fornix bundles).

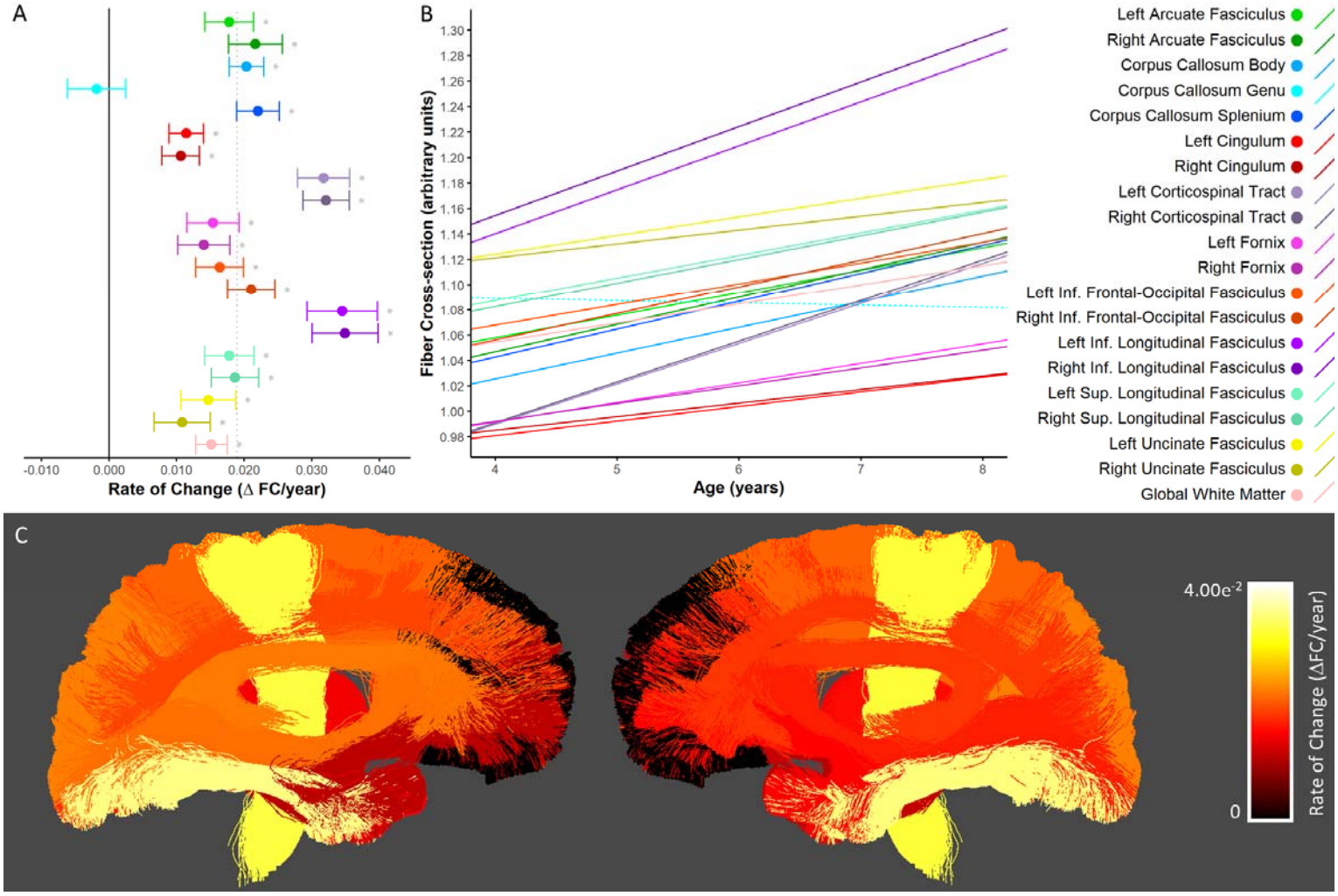

Figure 3. Developmental changes in fiber cross-section. A) Rate of change in FC shown for each tract. * denotes tracts in which there was significant growth. The solid black vertical line indicates zero change, while the dotted gray vertical line indicates the mean rate of change across all tracts. B) Linear trajectories of FC growth for each tract. Solid lines indicate tracts in which there was a statistically significant relationship with age; dotted lines correspond to non-significant tracts. C) Anatomical visualization of tract-wise rates of change in FC. Streamlines corresponding to each tract are coloured according to the rate of change of FC observed in that tract. Streamlines belonging to tracts in which the rate of change was not significantly greater then zero were assigned a value of zero and appear black in the figure.

Fiber Density and Cross-section (FDC)

Significant increases in FDC were seen for all tracts except for the genu of the corpus callosum, the uncinate fasciculi and the left superior longitudinal fasciculus (Figure 4A-B). Across tracts with statistically significant growth, the rate of change was most rapid in the corticospinal tract bilaterally, and slowest in the right superior longitudinal fasciculus. FDC increased 6.9-21.6% across those tracts with significant growth (Supplementary Table 4), with the greatest percent increases in the corticospinal tracts, and the smallest percent increase in the right superior longitudinal fasciculus. Rate of change was generally more rapid in tracts that connect to posterior regions of the brain (i.e. the splenium and inferior longitudinal fasciculi), and slower or non-significant in tracts that make connections to the frontal cortex (i.e. the uncinate fasciculi, superior longitudinal fasciculi, and genu of the corpus callosum; Figure 4C).

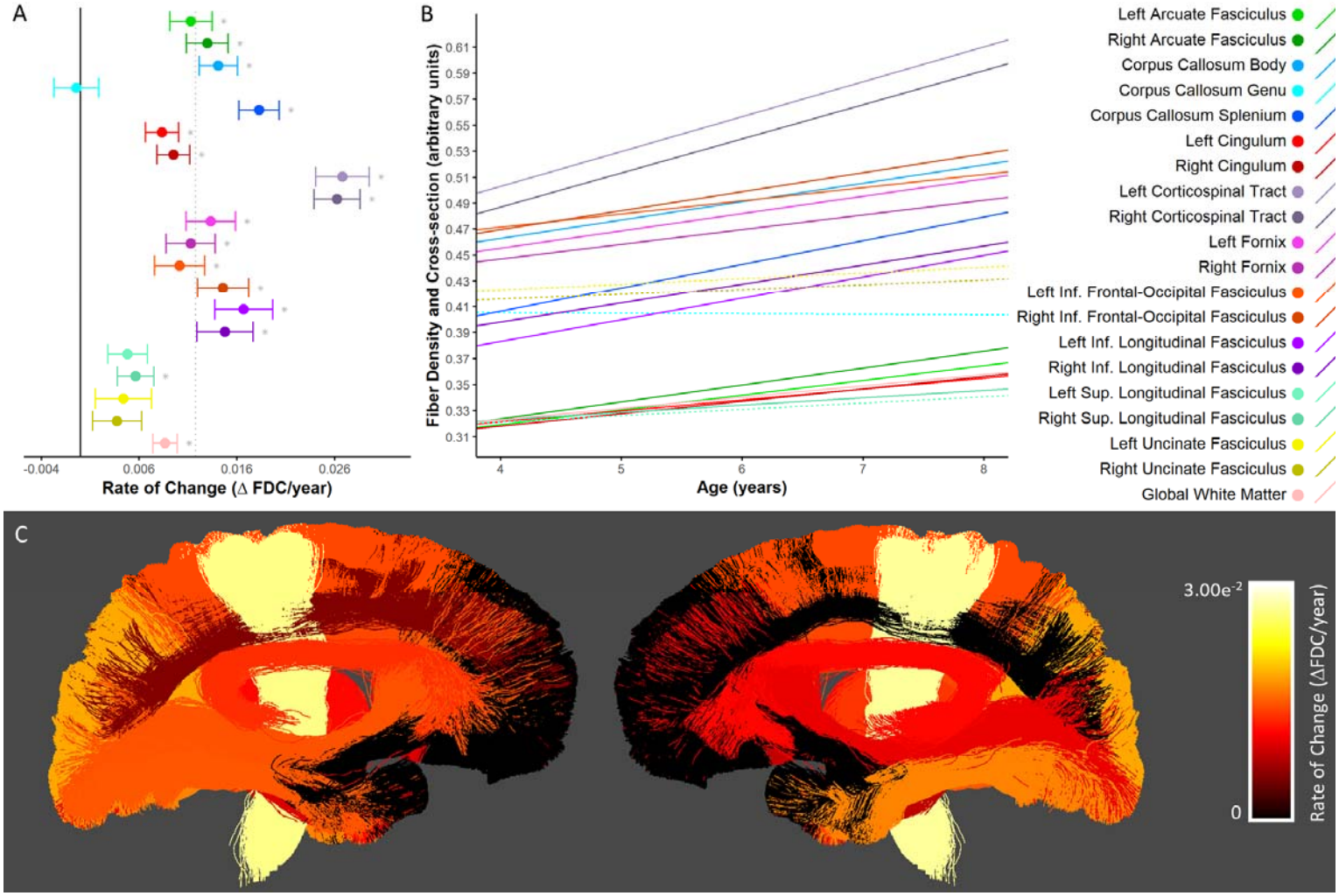

Figure 4. Developmental changes in fiber density and cross-section. A) Rate of change in FDC shown for each tract. * denotes tracts in which there was significant growth. The solid black vertical line indicates zero change, while the dotted gray vertical line indicates the mean rate of change across all tracts. B) Linear trajectories of FDC growth for each tract. Solid lines indicate tracts in which there was a statistically significant relationship with age; dotted lines correspond to non-significant tracts. C) Anatomical visualization of tract-wise rates of change in FDC. Streamlines corresponding to each tract are coloured according to the rate of change of FDC observed in that tract. Streamlines belonging to tracts in which the rate of change was not significantly greater then zero were assigned a value of zero and appear black in the figure.

Fractional Anisotropy

Similar to previous work (reviewed in (Lebel and Deoni 2018)), developmental increases in FA were observed in all major white matter tracts, as well as the global white matter mask (Figure 5A-B). Rates of FA increase were highly comparable across tracts; increases were slightly more rapid in the corticospinal tract and inferior frontal-occipital fasciculi, and slightly slower in the genu of the corpus callosum and the uncinate fasciculi. Percentage increases ranged from 2.0-7.6% and were largest in the right arcuate fasciculus and smallest in the right uncinate fasciculus (Supplementary Table 5). Spatially, rates of change were somewhat faster in posterior/superior tracts, and slower in tracts that connected to anterior/inferior brain regions such as the frontal and temporal lobes (i.e. the uncinate fasciculi, genu of the corpus callosum and inferior longitudinal fasciculi; Figure 5C).

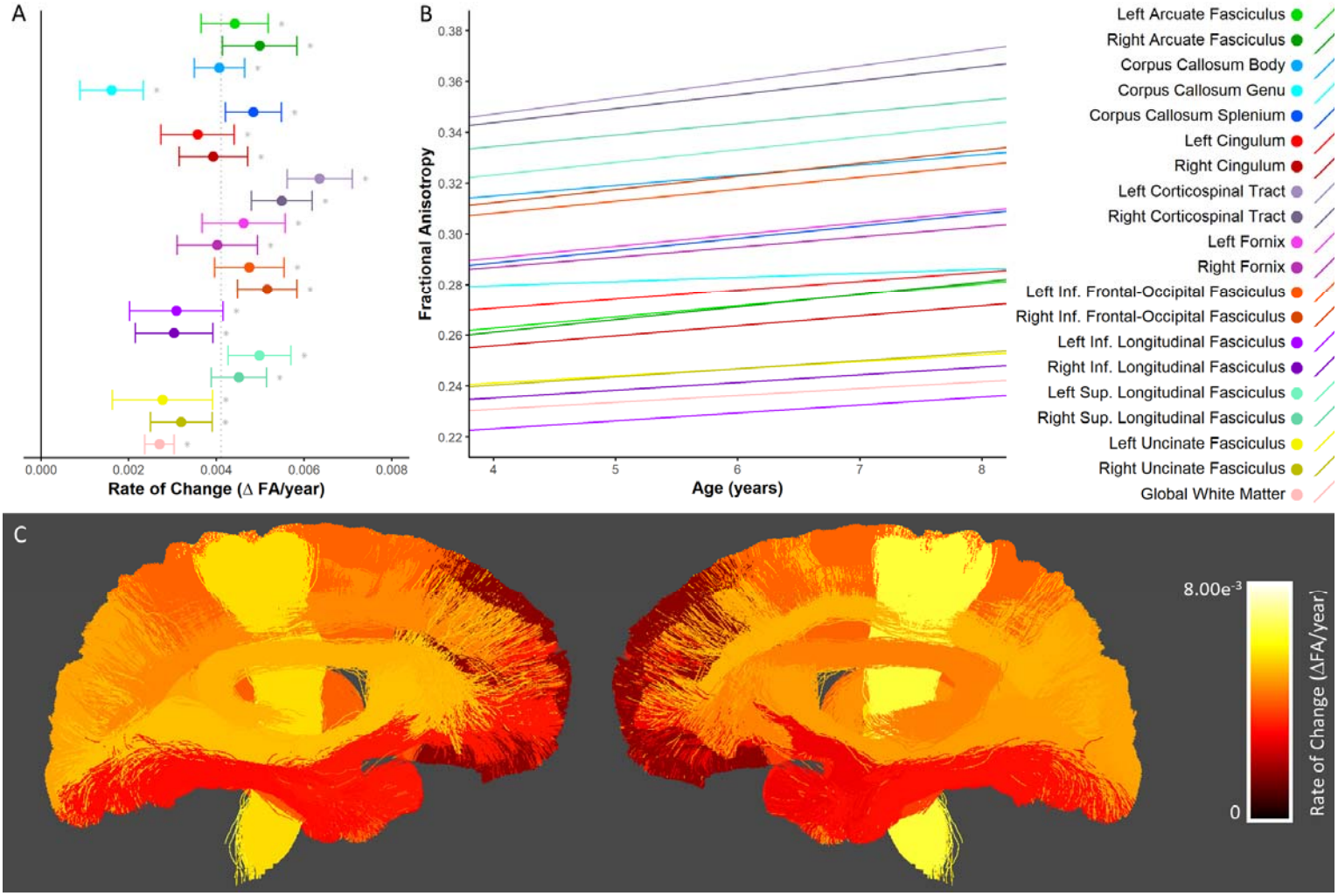

Figure 5. Developmental changes in fractional anisotropy. A) Rate of change in FA shown for each tract. * denotes tracts in which there was significant growth. The solid black vertical line indicates zero change, while the dotted gray vertical line indicates the mean rate of change across all tracts. B) Linear trajectories of FA growth for each tract. Solid lines indicate tracts in which there was a statistically significant relationship with age; dotted lines correspond to non-significant tracts. C) Anatomical visualization of tract-wise rates of change in FA. Streamlines corresponding to each tract are coloured according to the rate of change of FA observed in that tract.

Mean Diffusivity

Consistent with the literature (reviewed in (Lebel and Deoni 2018)), significant MD decreases were observed in all tested white matter tracts, as well as the global white matter mask (Figure 6A-B). Both absolute rates of change and percent changes were highly uniform across all tracts. Percentage decreases in MD ranged from 3.9-6.4% (Supplementary Table 6). Contrary to other metrics, MD of tracts in anterior/inferior regions, such as those in the frontal and temporal lobes (i.e. the uncinate fasciculi, inferior longitudinal fasciculi, inferior frontal-occipital fasciculi, and genu of the corpus callosum) changed relatively faster than tracts in posterior/superior brain regions (Figure 6C).

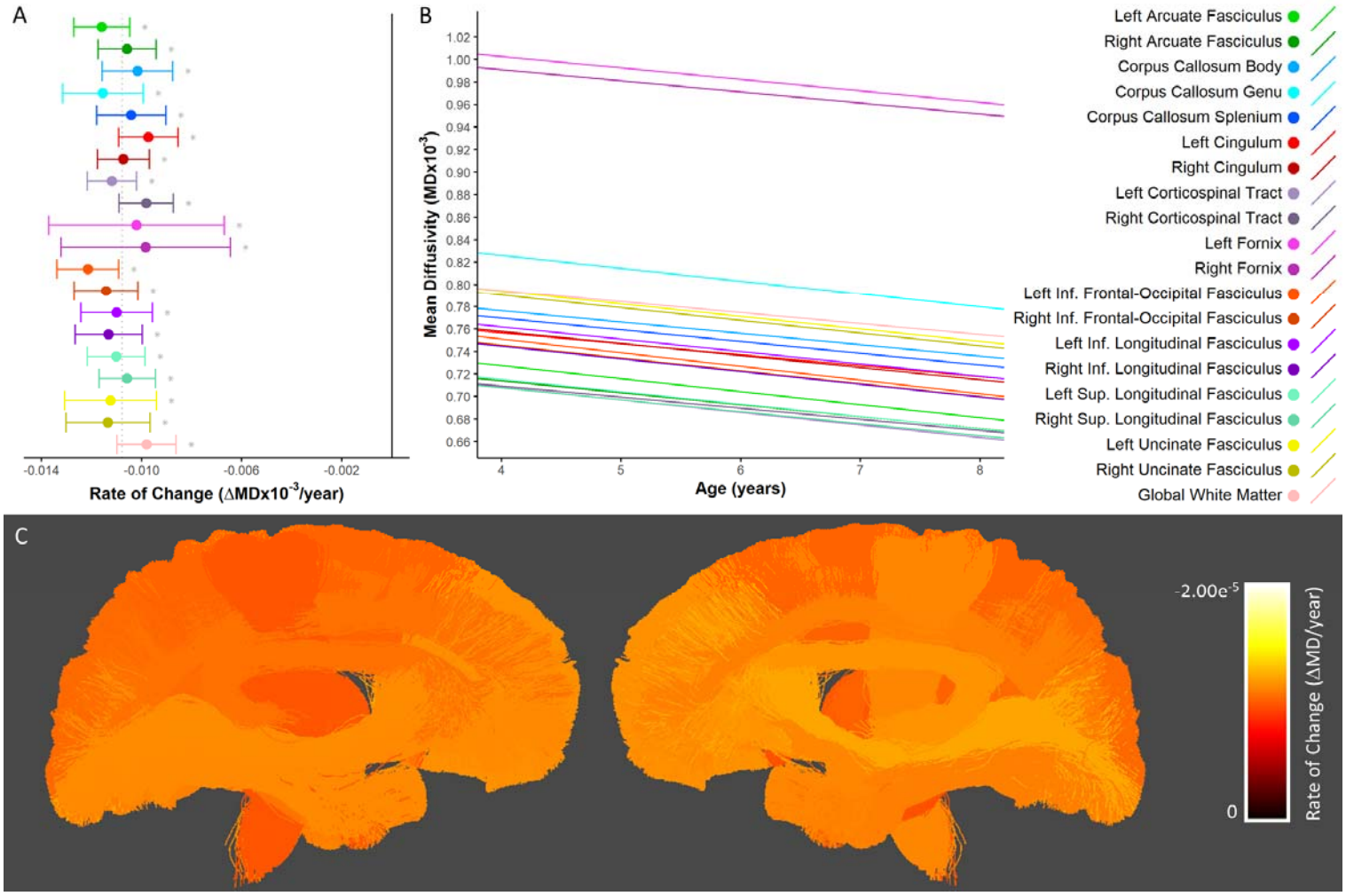

Figure 6. Developmental changes in mean diffusivity. A) Rate of change in MD shown for each tract. * denotes tracts in which there was significant growth. The solid black vertical line indicates zero change, while the dotted gray vertical line indicates the mean rate of change across all tracts. B) Linear trajectories of MD growth for each tract. Solid lines indicate tracts in which there was a statistically significant relationship with age; dotted lines correspond to non-significant tracts. C) Anatomical visualization of tract-wise rates of change in MD. Streamlines corresponding to each tract are coloured according to the rate of change of MD observed in that tract.

Aggregating Results Across Metrics

Figure 7 depicts tract-wise metrics, z-scored within each metric, to facilitate visualization of maturation patterns across metrics. Percent increases across metrics are shown in Supplementary Figure 2. Figure 7A shows that across all metrics, more rapid changes were observed in the corticospinal tracts, the right inferior frontal-occipital fasciculus and the splenium of the corpus callosum, while slower maturation was found in the genu of the corpus callosum, the global white matter mask, and the uncinate fasciculi. While some tracts showed consistently fast or slow maturation across metrics (e.g. consistently fast maturation in the left corticospinal tract, and consistently slow maturation in the global white matter mask), most tracts had variable rates of maturation across the various imaging metrics (e.g. the fornix bundles, inferior longitudinal fasciculi, and superior longitudinal fasciculi). Interestingly, for some tracts maturation of one imaging metric was vastly different than that of the other four (e.g. the left inferior frontal-occipital fasciculus and inferior longitudinal fasciculi, which matured particularly rapidly in MD and FC respectively). Spatially, incorporating data across all metrics tested, more rapid maturation was seen in tracts connecting to posterior/inferior brain regions (e.g. the splenium of the corpus callosum, corticospinal tracts and inferior longitudinal fasciculi), while slower maturation was seen in tracts connecting to the frontal cortex (e.g. the genu of the corpus callosum, the uncinate fasciculi and the superior longitudinal fasciculi; Figure 7B).

A notable observation from Figure 7A is that MD appears to have an opposite trend relative to other metrics within some tracts (despite negation of MD z-scores); the genu of the corpus callosum and uncinate fasciculus matured rapidly with respect to MD but slowly with respect to other metrics, the corticospinal tract and splenium of the corpus callosum show the opposite trend, with slow MD maturation and rapid maturation of FD, FC, FDC and FA. While this might suggest that MD maturation follows a distinct pattern compared to the maturation of other metrics, it is important to note that there was less variability in rates of change in MD compared to other metrics. In fact, in terms of absolute

rates of change, the fastest changes and highest variability within a single metric was seen in FC, while the largest percent increase was seen in FDC (Supplementary Figure 2). Because rates of change were rather consistent across tracts for MD, we provide an additional plot of across-metric changes where MD is not included (Figure 7C). Without MD, maturational rates across metrics appear to be more uniform, though it remains apparent that some tracts have more variability than others; the bilateral inferior longitudinal fasciculus and superior longitudinal fasciculus have large degrees of variability of maturational rates across metrics, while the body of the corpus callosum, bilateral arcuate fasciculus, right inferior frontal-occipital fasciculus and bilateral corticospinal tract appear to mature more homogenously. Spatial growth trends remain generally unchanged with exclusion of MD (Figure 7D).

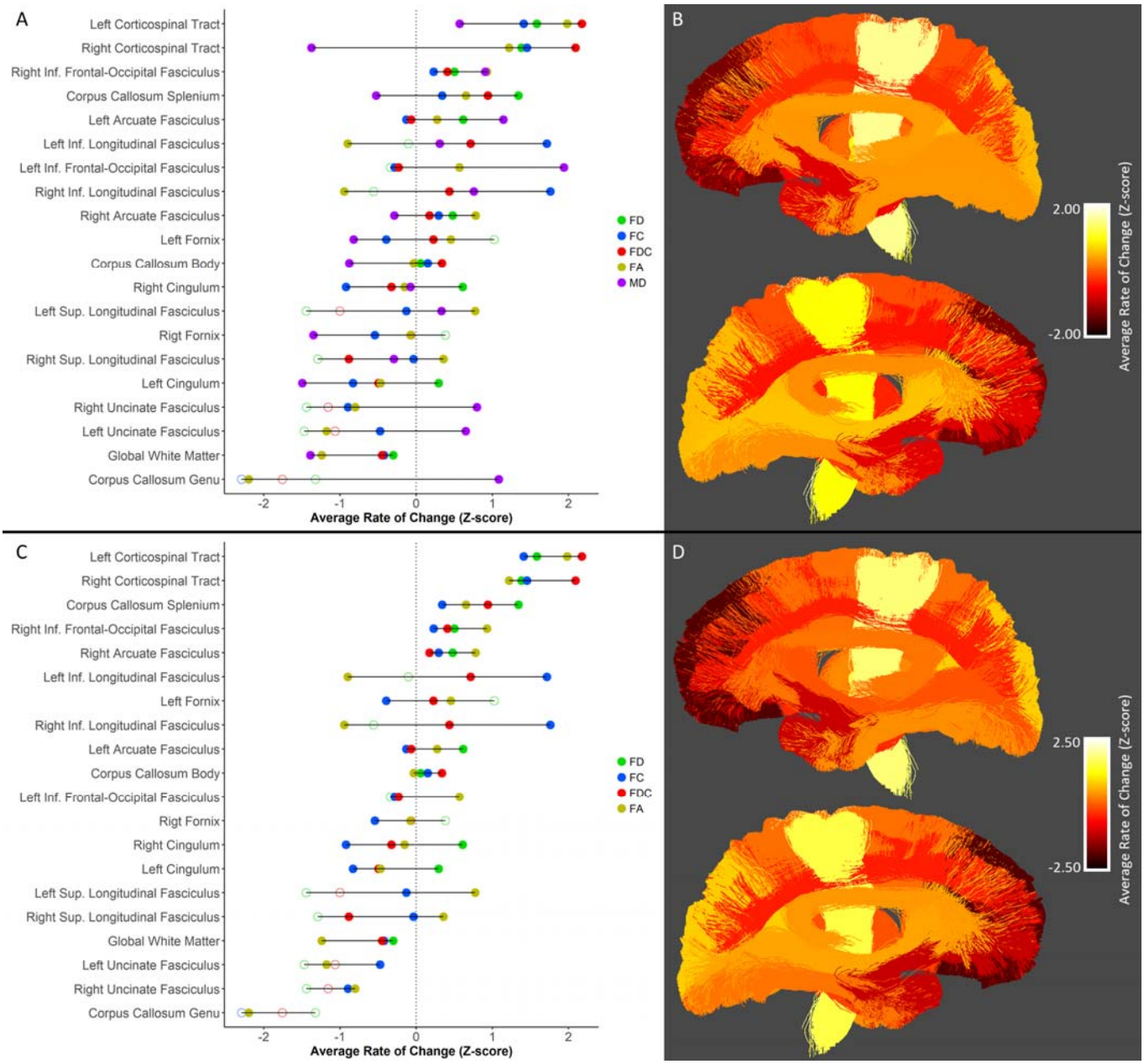

Figure 7: Metric-wise z-scored tract maturation, with and without inclusion of mean diffusivity. A) Tract-wise rate of change across FD, FC, FDC, FA and MD. Z-scores were calculated across tracts for each metric. Tracts are listed in descending order of average z-scored rate of change. Solid circles indicate statistically significant rates of change, while open circles indicate non-significant rates of change. The dotted gray line indicates the average rate of change across metrics (i.e. a z-score equal to zero). B) Anatomical visualization of tract-wise average z-scored rate of change across FD, FC, FDC and FA. In both panels, a negative z-score indicates a below average maturational rate, while a positive z-score indicates an above average maturational rate. C-D) Identical panels to A-B with MD excluded.

DISCUSSION

In the current study we investigated age-related changes in fixel-based quantitative metrics and compared developmental trajectories to historically utilized DTI metrics. We found that fiber density (FD) increased in several (but not all) major white matter tracts, while fiber cross-section (FC) increased in all tracts but one. Combined micro- and macro-structural growth (fiber density and cross-section (FDC)) was observed in most tracts. These findings suggest that early childhood white matter development is characterized by relatively widespread increases in cross-sectional fiber bundle size, with additional localized increases in axonal density. These developmental changes were observed alongside significantly increasing FA and decreasing MD in all tracts. Importantly, tracts exhibited unique developmental trajectories within and across metrics, providing further evidence that white matter maturation during early childhood is heterochronous. Furthermore, across all metrics except for MD we observed a posterior-anterior maturational trend with faster maturation of tracts in posterior brain regions and slower maturation of frontal tracts.

Fixel-based Metrics

White matter development during childhood is believed to be primarily driven by changes in axonal packing (Lebel and Deoni 2018). This is based in part on recent evidence that neurite density index (NDI), a proxy for axonal packing, shows widespread increases during childhood and adolescence that are associated with age more strongly than DTI metrics FA and MD (Genc, Malpas, et al. 2017; Mah et al. 2017). Here we see similar regional trends to those of NDI studies, with faster FD maturation in the corticospinal tract and splenium of the corpus callosum (Chang et al. 2015; Jelescu et al. 2015) and high relative changes in the cingulum bundles and arcuate fasciculi (Mah et al. 2017). Our findings are also consistent with longitudinal FBA analyses in older children (aged 9-13), showing FD increases with age in several WM tracts, including the corpus callosum, cingulum bundles, superior longitudinal fasciculi,

inferior frontal-occipital fasciculi and corticospinal tracts (Genc, Smith, et al. 2018; Genc et al. 2019). However, our FD findings are less widespread than we hypothesized: we report no significant FD increases in the genu of the corpus callosum, fornix, inferior longitudinal fasciculi, superior longitudinal fasciculi, or uncinate fasciculi. Although we find less widespread FD changes, some are larger in magnitude than that reported in older children (3.1-7.1% as compared to 2.5-3.5% reported by (Genc, Smith, et al. 2018)). Together, these findings suggest that axonal density changes during early childhood may be characterized by profound increases in select tracts (e.g. the splenium of the corpus callosum and corticospinal tracts) and increases in frontal-temporal tracts (e.g. the uncinate fasciculi and genu of the corpus callosum) may occur at a faster rate later in childhood. It is important to note however that while FD and NDI are both believed to be sensitive to axonal packing/density, differences in our results as compared to that of previous NDI studies (Chang et al. 2015; Genc, Malpas, et al. 2017; Mah et al. 2017; Genc, Smith, et al. 2018) may be in part due to differences in the underlying models used to derive these metrics. Further studies will therefore be necessary to validate our and these findings in relation to one another.

In addition to microstructural changes, a large number of structural (T1-weighted MRI) studies have shown developmental increases in white matter volumes from birth to adulthood (Lebel et al. 2008, 2012; Groeschel et al. 2010; Lebel and Beaulieu 2011; Taki et al. 2013). Volumes of individual major white matter tracts have also been shown to increase with age, with each tract following a unique developmental trajectory (Lebel and Beaulieu 2011; Lebel et al. 2012). Tract volume (Brouwer et al. 2012; Taki et al. 2013) and fiber cross-section (Genc, Smith, et al. 2018; Genc et al. 2019) have been shown to increase during childhood in most major white matter tracts, with slower maturation in the genu of the corpus callosum and uncinate fasciculi (Taki et al. 2013; Genc, Smith, et al. 2018); findings that are consistent with our FC results. Our group has also previously shown, in an independent dataset, directional selectivity in age-associations of white matter volumes: a superior-inferior oriented white

mater region encompassing the corticospinal tracts showed the largest age-slope in early childhood (Bray et al. 2015). This is consistent with the rapid FC changes in the CST reported here. Overall, our FC results suggest that early childhood is a particularly important period for development of the inferior longitudinal fasciculi and corticospinal tracts; while slower maturation in the uncinate fasciculi and superior longitudinal fasciculi, and no significant FC changes in the genu of the corpus callosum, may suggest later maturation of these tracts. It is also worth noting that FC changes were both more widespread, and showed larger percentage increases, than changes in FD. This suggests that while concurrent increases in axonal packing and fiber cross-section are prominent during early childhood (as evident from the large percentage changes observed in FDC), increases in fiber bundle size may be the primary driving factor of white matter maturation during this period.

DTI Metrics

To compare our FBA results to that of commonly utilized DTI metrics, we additionally assessed longitudinal changes in FA and MD as part of this study. Unsurprisingly, we observed developmental increases in FA and decreases in MD in all major white matter tracts; findings that are consistent with a large body of literature (see (Lebel and Deoni 2018) for review). Across the lifespan, tract maturation in terms of FA and MD has been shown to occur earliest for commissural and projection fibers, followed by association fibers, and then frontal-temporal projections (Westlye et al. 2010; Lebel and Beaulieu 2011; Lebel et al. 2012). This is broadly consistent with our results: for FA we find that changes are more rapid in projection fibers (i.e. the corticospinal tract) and slower in frontal-temporal fibers (e.g. the uncinate fasciculi); for MD we find that commissural projections change slightly more rapidly (e.g. the splenium of the corpus callosum) and that association fibers change at a rate comparable to the rest of the white matter.

Our results are also broadly consistent with studies that have investigated DTI metric changes from early childhood to early adulthood (Taki et al. 2013; Reynolds et al. 2019), though here we note some differences. A large DTI study in children aged 2-8 years similarly found rapid FA changes in the inferior frontal-occipital fasciculi with slower maturation in the uncinate fasciculi and genu of the corpus callosum (Reynolds et al. 2019). However, in contrast to our findings, they found that maturation of the corticospinal tract and splenium of the corpus callosum was slower than most other tracts. This may be attributed to the wider age range of participants in their study, or sex differences in white matter development (as our study included females only). Rapid changes in DTI metrics in the corticospinal tracts (Taki et al. 2013) and splenium (Brouwer et al. 2012) have been shown in early childhood to early adulthood, which might suggest that maturation in these tracts is more rapid in mid-late childhood than in very early childhood.

Fixel-based vs DTI Metrics

Unsurprisingly, we observed overlapping developmental changes in FBA and DTI metrics, suggesting that the underlying white matter maturation leads to observation of similar spatial patterns whether inferred from fixel-based quantitative measures or diffusion tensor-derived parameters. Across metrics, maturation followed a posterior-to-anterior spatial trend, with rapid maturation in the corticospinal tracts and splenium, and slower maturation in the genu of the corpus callosum and uncinate fasciculi. These findings are consistent with our hypothesis regarding spatial trends in tract-wise maturation, and are consistent with trends reported in the literature (Lebel et al. 2008, 2012; Lebel and Beaulieu 2011; Reynolds et al. 2019). Despite similarities, however, we did observe important distinctions in FBA and DTI metric developmental trends: percentage changes in tensor metrics were both less variable between tracts, and smaller in magnitude, than those observed in fixel-based metrics. These findings suggest that changes in non-specific, voxel-aggregate metrics inferred from the tensor model that are influenced by many factors are smaller in magnitude and more homogenous across

tracts during early childhood than changes in fixel-specific metrics that are sensitized to more specific biological properties. This suggests that FBA is better suited to tracking longitudinal changes in white matter maturation during early childhood, and may in turn be better able to identify white matter abnormalities in individuals with neurodevelopmental disorders (Dimond et al. 2019).

Interestingly, tracts displayed varying degrees of uniformity in maturational rates across all metrics: the inferior longitudinal fasciculi and superior longitudinal fasciculi had large degrees of variability, while the body of the corpus callosum, arcuate fasciculi, right inferior frontal-occipital fasciculus and corticospinal tracts matured at a relatively consistent rate across metrics. This might suggest multifaceted structural maturation is more coupled in some tracts than others, though this has yet to be explicitly tested and the implications of this remain unclear. While DTI metrics have been linked to histological white matter properties (Seehaus et al. 2015), the direct link between FBA metrics and cellular properties has not been robustly validated. Future studies should examine the underlying biological properties measured by fixel-based metrics, as well as potential mechanisms for coupling of white matter structural maturation and how concurrent and non-concurrent growth influences structural connectivity and brain function.

Cognitive-Behavioral and Functional Relevance

Early childhood is a period of profound maturation of cognitive and behavioral skills, including attention (Breckenridge et al. 2013; Mullane et al. 2016), working memory (Burnett Heyes et al. 2012), reading (Ferretti et al. 2008), math (Garon-Carrier et al. 2018), and self-regulation (Montroy et al. 2016). These skills have been linked to white matter properties during childhood (Qiu et al. 2008; Van Eimeren et al. 2008; Klarborg et al. 2013; Jolles et al. 2016; Bathelt et al. 2018), though the relationship between cognitive-behavioral skills and axonal density and fiber bundle size remains largely unexplored. One study has shown an association between FD and inattentive/internalizing behavior in typically

developing children (Genc et al. 2019), while we have previously reported an association between FD and social skills in adolescents and young adults with Autism Spectrum Disorder (Dimond et al. 2019). These findings open the possibility that fixel-metrics might explain cognitive capabilities in healthy individuals as well as relative deficits in individuals with neurodevelopmental disorders. Here we found that FD, FC, and FDC maturation was rapid in projection and commissural fibers (the corticospinal tracts and splenium), moderate in limbic tracts (the fornix and cingulum bundles), and slow or insignificant in frontal tracts (the genu, superior longitudinal fasciculi and uncinate fasciculi). These maturational trends may be related to rapid development of sensorimotor processes (Aboitiz and Montiel 2003; Welniarz et al. 2017), ongoing development of emotional regulation (Ahmed et al. 2015), and protracted development of executive functions (De Luca and Leventer 2011), respectively. We also observed rapid increases in FC of the inferior longitudinal fasciculi, which may be related to higher-order visual, emotional and reading capabilities (Herbet et al. 2018).

The mechanism by which individual differences in FD and FC might relate to cognitive-behavioral differences is unclear, though this is possibly mediated through influence on network connectivity in the brain. Increased axonal packing and fiber bundle size likely contribute to increases in structural connectivity over the course of neurodevelopment (Hagmann et al. 2010; Dennis et al. 2013), which may be related to developmental increases in functional network connectivity (Hagmann et al. 2010; Bennett and Rypma 2013), though the relationship between these metrics likely varies across the brain (Vazquez-Rodriguez et al. 2019). Work from our research group has demonstrated that functional network connectivity is strongly associated with age during early childhood (Rohr et al. 2017, 2018; Long et al. 2017). We have also previously shown that such functional connectivity is associated with cognitive skills such as attention in the same sample of participants as used in the current study (Rohr et al. 2017, 2018, 2019). Together, this research provides a potential theoretical framework to explain the interplay between structural, functional and cognitive development. Future longitudinal studies will

hopefully provide insight into the relationship between fiber density and fiber cross-section changes during early childhood, developmental increases in structural and functional brain connectivity, and cognition-behavioral maturation in typical and atypical neurodevelopment.

Strengths and Limitations

Strengths of the current study include a relatively large sample size, and mitigation of potential confounding effects of motion through careful data screening, correction during preprocessing, and regression of motion in statistical analyses. Though we utilized a slightly lower b-value than is generally recommended for CSD (Tournier et al. 2013) and quantification of fiber density (Raffelt, Tournier, Rose, et al. 2012), our study made use of state-of-the-art "single-shell 3-tissue CSD" (SS3T-CSD; (Dhollander and Connelly 2016)), which is capable of isolating the diffusion signal attributable to white matter by modelling and removing the contribution from grey matter and CSF (Dhollander et al. 2017).

One limitation of the current study is our exclusive use of female participants, which blinds us to any potential sex differences in white matter development. The data utilized here are part of an ongoing study investigating brain abnormalities in Turner syndrome, a disorder that only affects females; hence typically-developing control participants recruited for this study were correspondingly exclusively girls. While evidence for sex differences in white matter maturation is mixed (see (Lebel and Deoni 2018) for recent review), some studies point towards small but significant sex difference in DTI (Reynolds et al. 2019) and FBA metrics (Genc, Seal, et al. 2017). Additionally, while we tested exclusively for linear trends in white matter maturation, a recent DTI study has shown that FA and MD of select tracts follow quadratic trajectories over early childhood (Reynolds et al. 2019). Given the narrow age and limited number of scans (1-3) for each participant in our study, our sensitivity to non-linear trends would have been limited.

Conclusion

Here we report widespread developmental increases in tract-wise fiber cross-section between the ages of 4-8 years, with additional increases in fiber density within specific tracts. Combined micro- and macro-structural growth (FDC) demonstrated the greatest percentage changes over this age range, while fixel-based metrics in general showed both greater percentile changes, and greater between-tract variability, than voxel-based DTI metrics. These findings highlight early childhood as a period of dynamic white matter maturation, characterized primarily by developmental changes in fiber bundle size, with moderate changes in axonal packing density, and ongoing, albeit less pronounced changes in DTI properties. Our results add to the understanding of, and help to bridge gaps in, the characterization of white matter development from birth to adulthood and demonstrate the utility of FBA in this neurodevelopmental context.

FUNDING

This work was supported by a graduate studentship from Alberta Innovates Health Solutions, an Alexander Graham Bell Canada Graduate Scholarship from the Natural Sciences and Engineering Research Council of Canada (NSERC), a Michael Smith Foreign Study Supplement from NSERC, and RHISE HBI-Melbourne Trainee Research Exchange funding awarded to D.D. This work was supported by an NSERC Discovery Award, CIHR-INMHA Bridge Award and CIHR Project to SB.

ACKNOWLEDGEMENTS

We thank all the families who participated in this study, as well as staff at the Alberta Children's Hospital Imaging Centre.

REFERENCES

Aboitiz F, Montiel J. 2003. One hundred million years of interhemispheric communication: The history of the corpus callosum. Brazilian J Med Biol Res. 36:409-420.

Ahmed SP, Bittencourt-Hewitt A, Sebastian CL. 2015. Neurocognitive bases of emotion regulation development in adolescence. Dev Cogn Neurosci. 15:11-25.

Andersson JL, Graham MS, Zsoldos E, Sotiropoulos SN. 2016. Incorporating outlier detection and replacement into a non-parametric framework for movement and distortion correction of diffusion MR images. Neuroimage. 141:556–572.

Andersson JLR, Graham MS, Drobnjak I, Zhang H, Filippini N, Bastiani M. 2017. Towards a comprehensive framework for movement and distortion correction of diffusion MR images: Within volume movement. Neuroimage. 152:450–466.

Andersson JLR, Sotiropoulos SN. 2016. An integrated approach to correction for off-resonance effects and subject movement in diffusion MR imaging. Neuroimage. 125:1063–1078.

Bates D, Maechler M, Bolker B, Walker S, Christensen RHB, Singmann H, Dai B, Eigen C. 2017. lme4: Fitting linear mixed-effects models using lme4. J Stat Softw. 67:1–113.

Bathelt J, Gathercole SE, Johnson A, Astle DE. 2018. Differences in brain morphology and working memory capacity across childhood. Dev Sci. 21:1–13.

Bennett IJ, Rypma B. 2013. Advances in functional neuroanatomy: a review of combined DTI and fMRI studies in healthy younger and older adults. Neurosci Biobehav Rev. 37:1201–1210.

Bray S, Krongold M, Cooper C, Lebel C. 2015. Synergistic Effects of Age on Patterns of White and Gray Matter Volume across Childhood and Adolescence. eNeuro. 2: 1-13.

Breckenridge K, Braddick O, Atkinson J. 2013. The organization of attention in typical development: a new preschool attention test battery. Br J Dev Psychol. 31:271–288.

Brouwer RM, Mandl RCW, Schnack HG, van Soelen ILC, van Baal GC, Kahn RS, Pol HEH, Boomsma DI, Peper JS. 2012. White Matter Development in Early Puberty: A Longitudinal Volumetric and Diffusion Tensor Imaging Twin Study. PLoS One. 7:e32316.

Burnett Heyes S, Zokaei N, van der Staaij I, Bays PM, Husain M. 2012. Development of visual working memory precision in childhood. Dev Sci. 15:528–538.

Chang YS, Owen JP, Pojman NJ, Thieu T, Bukshpun P, Wakahiro ML, Berman JI, Roberts TP, Nagarajan SS, Sherr EH, Mukherjee P. 2015. White Matter Changes of Neurite Density and Fiber Orientation Dispersion during Human Brain Maturation. PLoS One. 10:e0123656.

De Luca CR, Leventer RJ. 2011. Developmental trajectories of executive functions across the lifespan. In: Executive Functions and the Frontal Lobes: A Lifespan Perspective. p. 23–56.

Dennis EL, Jahanshad N, McMahon KL, de Zubicaray GI, Martin NG, Hickie IB, Toga AW, Wright MJ, Thompson PM. 2013. Development of brain structural connectivity between ages 12 and 30: A 4-Tesla diffusion imaging study in 439 adolescents and adults. Neuroimage. 64:671-684.

Dhollander T, Connelly A. 2016. A novel iterative approach to reap the benefits of multi-tissue CSD from just single-shell (+ b = 0) diffusion MRI data. 24th International Society of Magnetic Resonance in Medicine. 24:3010.

Dhollander T, Raffelt D, Connelly A. 2016. Unsupervised 3-tissue response function estimation from single-shell or multi-shell diffusion MR data without a co-registered T1 image. Proceedings of ISMRM Workshop on Breaking the Barriers of Diffusion MRI. p. 5.

Dhollander T, Raffelt D, Connelly A. 2017. Towards interpretation of 3-tissue constrained spherical

deconvolution results in pathology. 25th International Society of Magnetic Resonance in Medicine. 25:1815.

Dimond D, Schuetze M, E. Smith R, Dhollander T, Cho I, Vinette S, Ten Eycke K, Lebel C, McCrimmon A, Dewey D, Connelly A, Bray S. 2019. Reduced White Matter Fiber Density in Autism Spectrum Disorder. Cereb Cortex. 29:1778-1788.

Ferretti G, Mazzotti S, Brizzolara D. 2008. Visual scanning and reading ability in normal and dyslexic children. Behav Neurol. 19:87–92.

Garon-Carrier G, Boivin M, Lemelin JP, Kovas Y, Parent S, Séguin J, Vitaro F, Tremblay RE, Dionne G. 2018. Early developmental trajectories of number knowledge and math achievement from 4 to 10 years: Low-persistent profile and early-life predictors. J Sch Psychol. 68:84–98.

Genc S, Malpas CB, Ball G, Silk TJ, Seal ML. 2018. Age, sex, and puberty related development of the corpus callosum: a multi-technique diffusion MRI study. Brain Struct Funct. 223:2753–2765.

Genc S, Malpas CB, Gulenc A, Sciberras E, Efron D. 2019. Longitudinal white matter development in children is associated with puberty , attentional difficulties , and mental health. bioRxiv. 607671.

Genc S, Malpas CB, Holland SK, Beare R, Silk TJ. 2017. Neurite density index is sensitive to age related differences in the developing brain. Neuroimage. 148:373–380.

Genc S, Seal ML, Dhollander T, Malpas CB, Hazell P, Silk TJ. 2017. White matter alterations at pubertal onset. Neuroimage. 156:286–292.

Genc S, Smith RE, Malpas CB, Anderson V, Nicholson JM, Efron D, Sciberras E, Seal ML, Silk TJ. 2018. Development of white matter fibre density and morphology over childhood: A longitudinal fixel-based analysis. Neuroimage. 183:666–676.

Groeschel S, Vollmer B, King MD, Connelly A. 2010. Developmental changes in cerebral grey and white matter volume from infancy to adulthood. Int J Dev Neurosci. 28:481–489.

Hagmann P, Sporns O, Madan N, Cammoun L, Pienaar R, Wedeen VJ, Meuli R, Thiran JP, Grant PE. 2010. White matter maturation reshapes structural connectivity in the late developing human brain. Proc Natl Acad Sci U S A. 107:19067–19072.

Herbet G, Zemmoura I, Duffau H. 2018. Functional Anatomy of the Inferior Longitudinal Fasciculus: From Historical Reports to Current Hypotheses. Front Neuroanat. 12:1–15.

Hrong-Tai Fai A, Cornelius PL. 2007. Approximate F-tests of multiple degree of freedom hypotheses in generalized least squares analyses of unbalanced split-plot experiments. J Stat Comput Simul. 54:363-378.

Jelescu IO, Veraart J, Adisetiyo V, Milla SS, Novikov DS, Fieremans E. 2015. One diffusion acquisition and different white matter models: How does microstructure change in human early development based on WMTI and NODDI? Neuroimage. 107:242–256.

Jenkinson M, Beckmann CF, Behrens TEJ, Woolrich MW, Smith SM. 2012. FSL. Neuroimage. 62:782-790.

Jeurissen B, Leemans A, Tournier JD, Jones DK, Sijbers J. 2013. Investigating the prevalence of complex fiber configurations in white matter tissue with diffusion magnetic resonance imaging. Hum Brain Mapp. 34:2747–2766.

Jeurissen B, Tournier JD, Dhollander T, Connelly A, Sijbers J. 2014. Multi-tissue constrained spherical deconvolution for improved analysis of multi-shell diffusion MRI data. Neuroimage. 103:411–426.

Jolles D, Wassermann D, Chokhani R, Richardson J, Tenison C, Bammer R, Fuchs L, Supekar K, Menon V. 2016. Plasticity of left perisylvian white-matter tracts is associated with individual differences in math learning. Brain Struct Funct. 221:1337–1351.

Klarborg B, Skak Madsen K, Vestergaard M, Skimminge A, Jernigan TL, Baaré WF. 2013. Sustained attention is associated with right superior longitudinal fasciculus and superior parietal white matter microstructure in children. Hum Brain Mapp. 34:3216–3232.

Kuznetsova A, Brockhoff PB, Christensen RHB. 2017. lmerTest Package: Tests in Linear Mixed Effects Models. J Stat Softw. 82:1-26.

Lebel C, Beaulieu C. 2011. Longitudinal development of human brain wiring continues from childhood into adulthood. J Neurosci. 31:10937–10947.

Lebel C, Deoni S. 2018. The development of brain white matter microstructure. Neuroimage. 182:207–218.

Lebel C, Gee M, Camicioli R, Wieler M, Martin W, Beaulieu C. 2012. Diffusion tensor imaging of white matter tract evolution over the lifespan. Neuroimage. 60:340–352.

Lebel C, Walker L, Leemans A, Phillips L, Beaulieu C. 2008. Microstructural maturation of the human brain from childhood to adulthood. Neuroimage. 40:1044–1055.

Long X, Benischek A, Dewey D, Lebel C. 2017. Age-related functional brain changes in young children. Neuroimage. 155:322–330.

Mah A, Geeraert B, Lebel C. 2017. Detailing neuroanatomical development in late childhood and early adolescence using NODDI. PLoS One. 12:1–16.

Montroy JJ, Bowles RP, Skibbe LE, McClelland MM, Morrison FJ. 2016. The development of self-regulation across early childhood. Dev Psychol. 52:1744–1762.

Mullane JC, Lawrence MA, Corkum P V, Klein RM, McLaughlin EN. 2016. The development of and interaction among alerting, orienting, and executive attention in children. Child Neuropsychol.

22:155–176.

Qiu D, Tan LH, Zhou K, Khong PL. 2008. Diffusion tensor imaging of normal white matter maturation from late childhood to young adulthood: Voxel-wise evaluation of mean diffusivity, fractional anisotropy, radial and axial diffusivities, and correlation with reading development. Neuroimage. 41:223–232.

R Core Team. 2014. R: A language and environment for statistical computing. R Found Stat Comput Vienna, Austria URL http//wwwR-project.org/.

Raffelt D, Dhollander T, Tournier JD, Tabbara R, Smith RE, Pierre E, Connelly A. 2017. Bias field correction and intensity normalisation for quantitative analysis of apparent fiber density. 25th International Society of Magnetic Resonance in Medicine. 25:3541.

Raffelt D, Tournier JD, Crozier S, Connelly A, Salvado O. 2012. Reorientation of fiber orientation distributions using apodized point spread functions. Magn Reson Med. 67:844–855.

Raffelt D, Tournier JD, Fripp J, Crozier S, Connelly A, Salvado O. 2011. Symmetric diffeomorphic registration of fibre orientation distributions. Neuroimage. 56:1171–1180.

Raffelt D, Tournier JD, Rose S, Ridgway GR, Henderson R, Crozier S, Salvado O, Connelly A. 2012. Apparent Fibre Density: a novel measure for the analysis of diffusion-weighted magnetic resonance images. Neuroimage. 59:3976–3994.

Raffelt DA, Smith RE, Ridgway GR, Tournier JD, Vaughan DN, Rose S, Henderson R, Connelly A. 2015. Connectivity-based fixel enhancement: Whole-brain statistical analysis of diffusion MRI measures in the presence of crossing fibres. Neuroimage. 117:40–55.

Raffelt DA, Tournier JD, Smith RE, Vaughan DN, Jackson G, Ridgway GR, Connelly A. 2017. Investigating white matter fibre density and morphology using fixel-based analysis. Neuroimage. 144:58–73.

Reynolds JE, Grohs MN, Dewey D, Lebel C. 2019. Global and regional white matter development in early childhood. bioRxiv. 524785.

Rohr CS, Arora A, Cho IYK, Katlariwala P, Dimond D, Dewey D, Bray S. 2018. Functional network integration and attention skills in young children. Dev Cogn Neurosci. 30:200-211.

Rohr CS, Dimond D, Schuetze M, Cho IYK, Lichtenstein-Vidne L, Okon-Singer H, Dewey D, Bray S. 2019. Girls' attentive traits associate with cerebellar to dorsal attention and default mode network connectivity. Neuropsychologia. 127:84–92.

Rohr CS, Vinette SA, Parsons KA, Cho IY, Dimond D, Benischek A, Lebel C, Dewey D, Bray S. 2017. Functional Connectivity of the Dorsal Attention Network Predicts Selective Attention in 4-7 year-old Girls. Cereb Cortex. 27: 4350-4360.

Seehaus A, Roebroeck A, Bastiani M, Fonseca L, Bratzke H, Lori N, Vilanova A, Goebel R, Galuske R. 2015. Histological validation of high-resolution DTI in human post mortem tissue. Front Neuroanat. 9:1–12.

Smith RE, Tournier JD, Calamante F, Connelly A. 2013. SIFT: Spherical-deconvolution informed filtering of tractograms. Neuroimage. 67:298–312.

Taki Y, Thyreau B, Hashizume H, Sassa Y, Takeuchi H, Wu K, Kotozaki Y, Nouchi R, Asano M, Asano K, Fukuda H, Kawashima R. 2013. Linear and curvilinear correlations of brain white matter volume, fractional anisotropy, and mean diffusivity with age using voxel-based and region-of-interest analyses in 246 healthy children. Hum Brain Mapp. 34:1842–1856.

Tournier J-D, Calamante F, Connelly A. 2010. Improved probabilistic streamlines tractography by 2nd order integration over fibre orientation distributions. Proc Int Soc Magn Reson Med. 88:2010.

Tournier J-D, Smith RE, Raffelt DA, Tabbara R, Dhollander T, Pietsch M, Christiaens D, Jeurissen B, Yeh C-

H, Connelly A. 2019. MRtrix3: A fast, flexible and open software framework for medical image processing and visualisation. bioRxiv. 551739.

Tournier JD, Calamante F, Connelly A. 2007. Robust determination of the fibre orientation distribution in diffusion MRI: non-negativity constrained super-resolved spherical deconvolution. Neuroimage. 35:1459–1472.

Tournier JD, Calamante F, Connelly A. 2013. Determination of the appropriate b value and number of gradient directions for high-angular-resolution diffusion-weighted imaging. NMR Biomed. 26:1775–1786.

Tustison NJ, Avants BB, Cook PA, Zheng Y, Egan A, Yushkevich PA, Gee JC. 2010. N4ITK: improved N3 bias correction. IEEE Trans Med Imaging. 29:1310–1320.

Van Eimeren L, Niogi SN, McCandliss BD, Holloway ID, Ansari D. 2008. White matter microstructures underlying mathematical abilities in children. Neuroreport. 19:1117–1121.

Vazquez-Rodriguez B, Suarex L., Shafiei G, Markello R., Paquola C, Hagmann P, van den Heuvel M., Bernhardt B., Spreng R., Misic B. 2019. Gradients of structure-function tethering across neocortex. bioRxiv. 561985.

Welniarz Q, Dusart I, Roze E. 2017. The corticospinal tract: Evolution, development, and human disorders. Dev Neurobiol. 77:810-829.

Westlye LT, Walhovd KB, Dale AM, Bjørnerud A, Due-Tønnessen P, Engvig A, Grydeland H, Tamnes CK, Østby Y, Fjell AM. 2010. Life-span changes of the human brain white matter: Diffusion tensor imaging (DTI) and volumetry. Cereb Cortex. 20:2055–2068.

Yeatman JD, Wandell BA, Mezer AA. 2014. Lifespan maturation and degeneration of human brain white matter. Nat Commun. 5:4932.

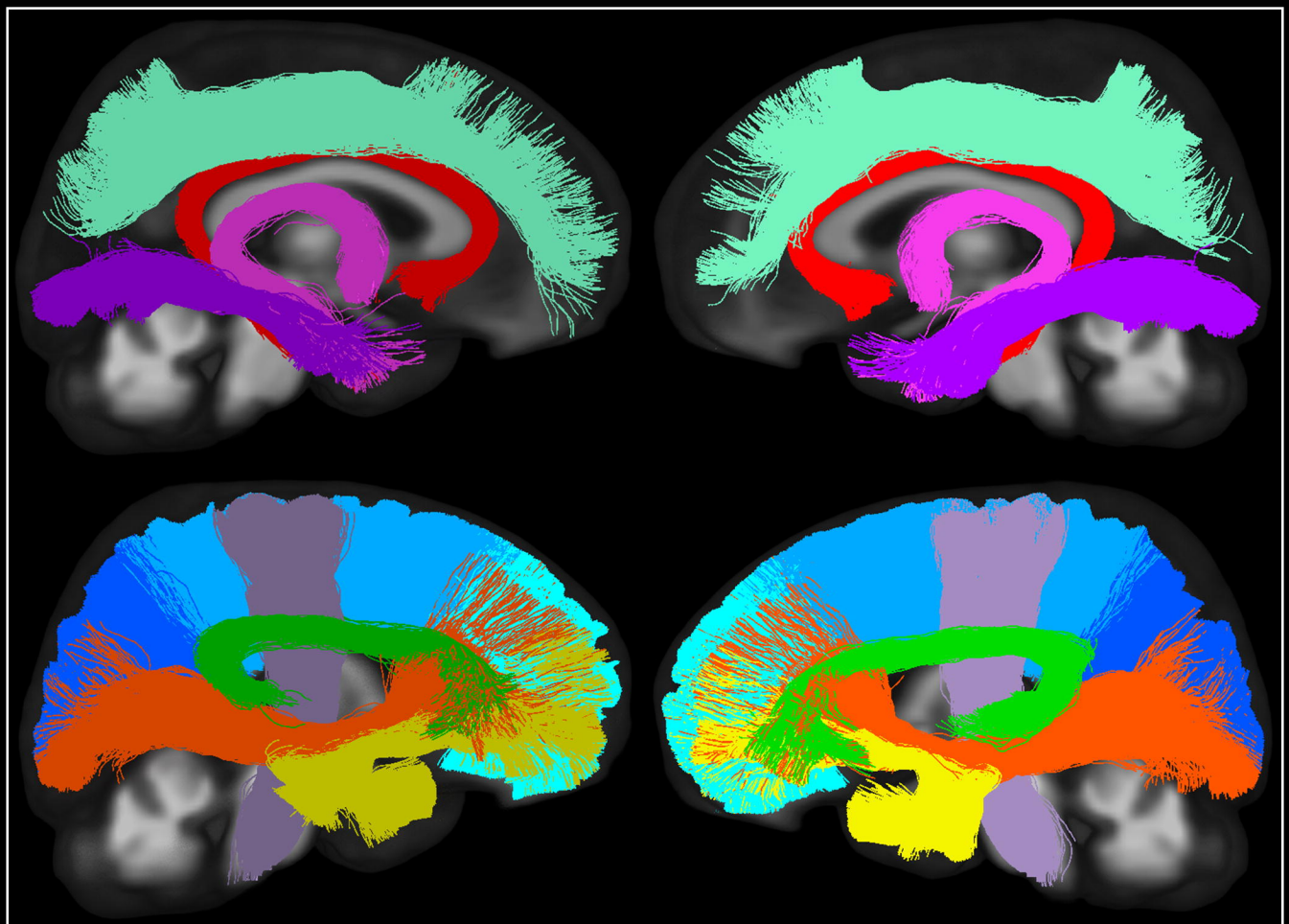

Superior longitudinal fasciculus

Inferior longitudinal fasciculus

Fornix

Cingulum

Corticospinal tract

Corpus callosum:

(genu, body, splenium)

Uncinate fasciculus

Arcuate fasciculus

Inferior frontal-occipital fasciculus

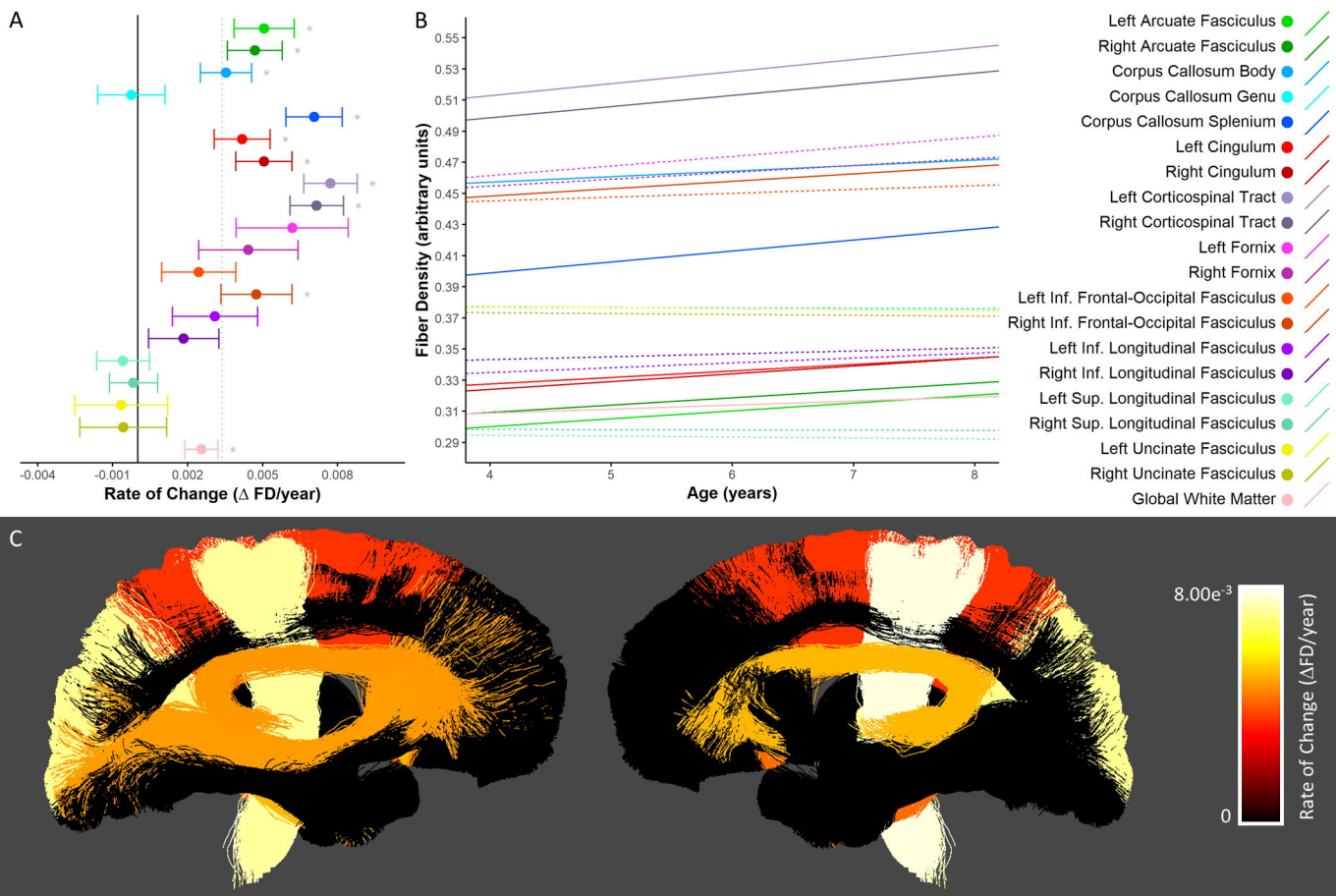
A
-0.004
-0.001
0.002
0.005
0.008
Rate of Change (Δ FD/year)
B
Fiber Density (arbitrary units)
0.55
0.53
0.51
0.49
0.47
0.45
0.43
0.41
0.39
0.37
0.35
0.33
0.31
0.29
4
5
6
7
8
Age (years)
Left Arcuate Fasciculus
Right Arcuate Fasciculus
Corpus Callosum Body
Corpus Callosum Genu
Corpus Callosum Splenium
Left Cingulum
Right Cingulum
Left Corticospinal Tract
Right Corticospinal Tract
Left Fornix
Right Fornix
Left Inf. Frontal-Occipital Fasciculus
Right Inf. Frontal-Occipital Fasciculus
Left Inf. Longitudinal Fasciculus
Right Inf. Longitudinal Fasciculus
Left Sup. Longitudinal Fasciculus
Right Sup. Longitudinal Fasciculus
Left Uncinate Fasciculus
Right Uncinate Fasciculus
Global White Matter
C
8.00e-3
0
Rate of Change (ΔFD/year)

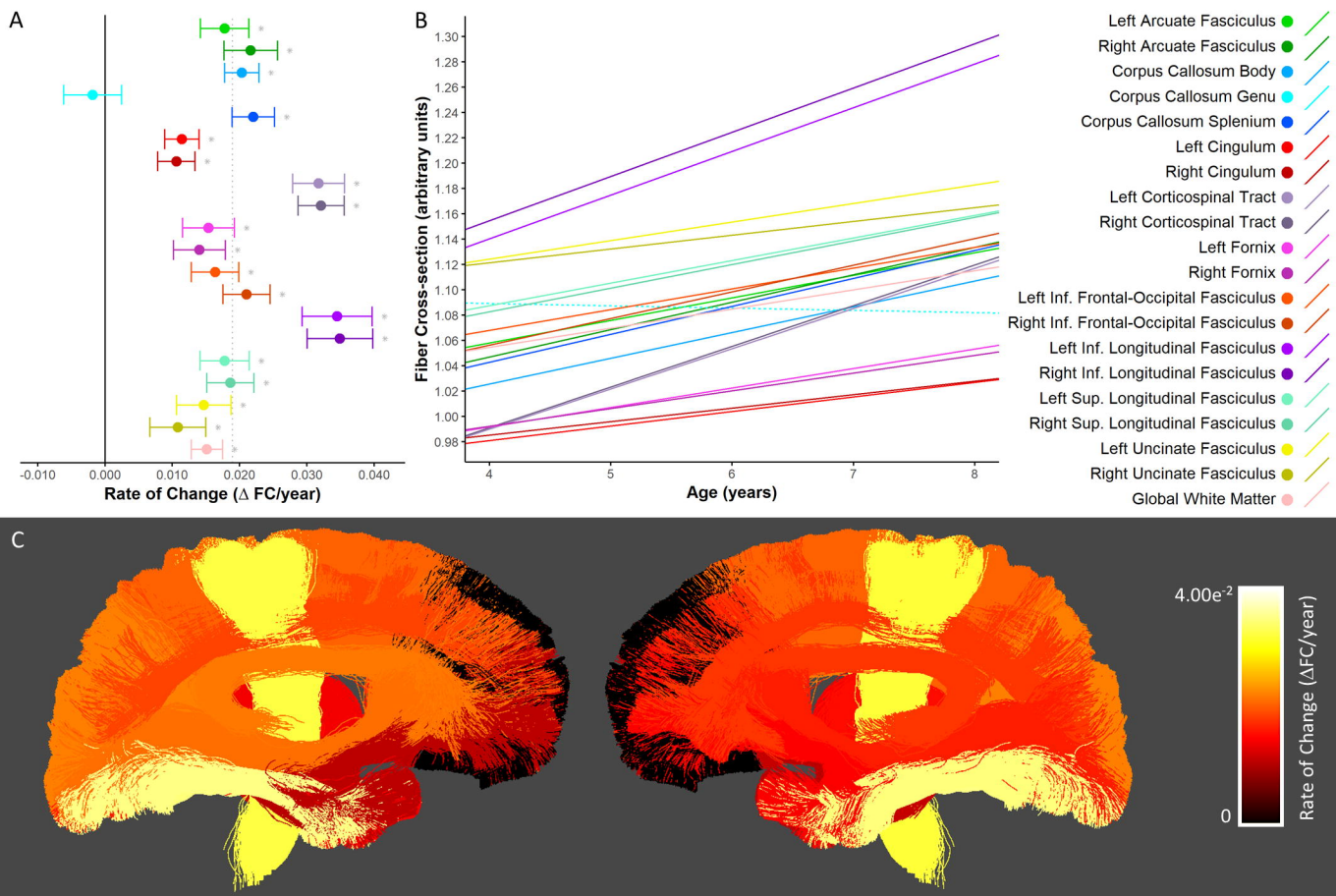
A
-0.010
0.000
0.010
0.020
0.030
0.040
Rate of Change (Δ FC/year)
B
Fiber Cross-section (arbitrary units)
1.30
1.28
1.26
1.24
1.22
1.20
1.18
1.16
1.14
1.12
1.10
1.08
1.06
1.04
1.02
1.00
0.98
4
5
6
7
8
Age (years)
Left Arcuate Fasciculus
Right Arcuate Fasciculus
Corpus Callosum Body
Corpus Callosum Genu
Corpus Callosum Splenium
Left Cingulum
Right Cingulum
Left Corticospinal Tract
Right Corticospinal Tract
Left Fornix
Right Fornix
Left Inf. Frontal-Occipital Fasciculus
Right Inf. Frontal-Occipital Fasciculus
Left Inf. Longitudinal Fasciculus
Right Inf. Longitudinal Fasciculus
Left Sup. Longitudinal Fasciculus
Right Sup. Longitudinal Fasciculus
Left Uncinate Fasciculus
Right Uncinate Fasciculus
Global White Matter
C
4.00e-2
0
Rate of Change (ΔFC/year)

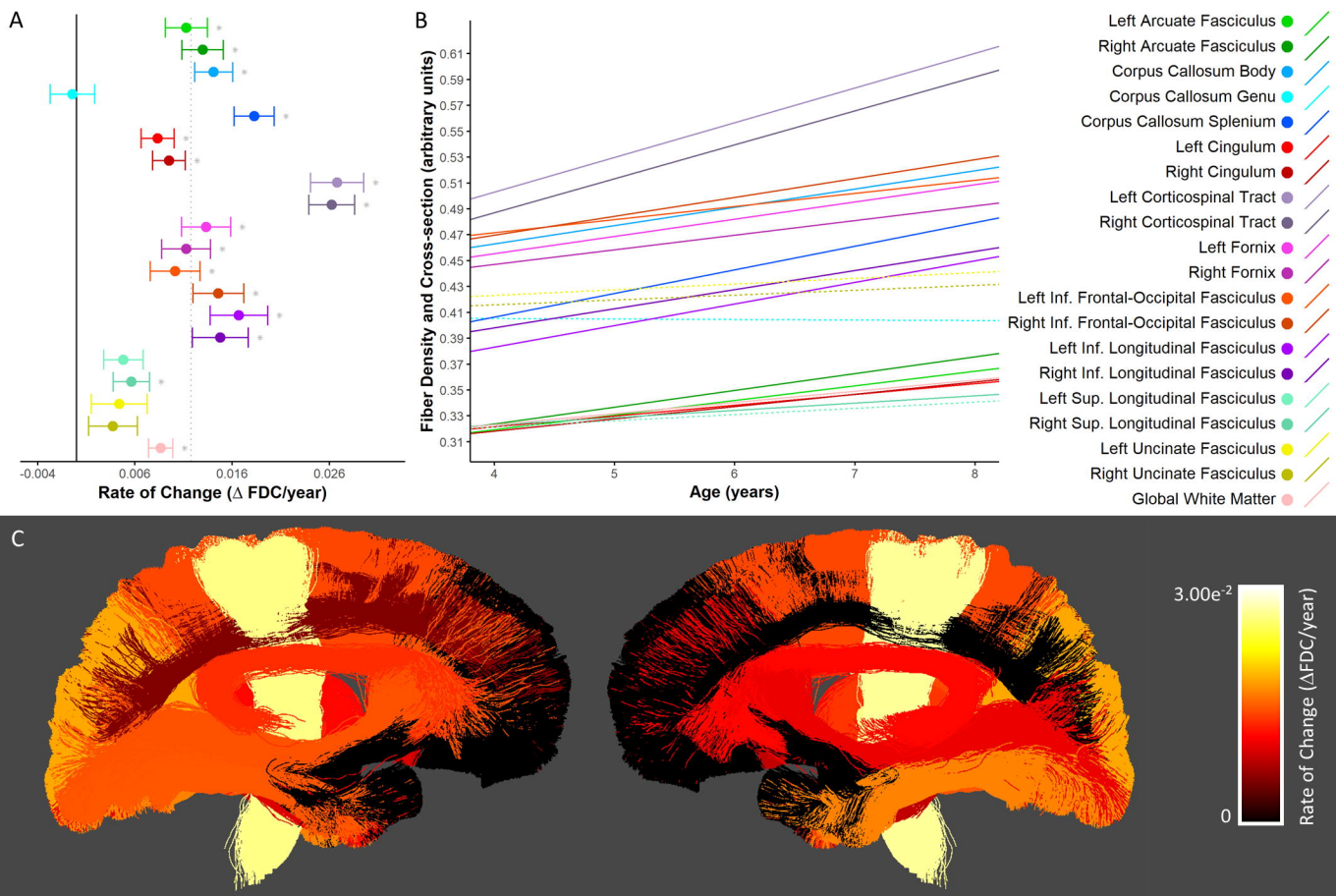
A
-0.004
0.006
0.016
0.026
Rate of Change (Δ FDC/year)
B
Fiber Density and Cross-section (arbitrary units)
0.61
0.59
0.57
0.55
0.53
0.51
0.49
0.47
0.45
0.43
0.41
0.39
0.37
0.35
0.33
0.31
4
5
6
7
8
Age (years)
Left Arcuate Fasciculus
Right Arcuate Fasciculus
Corpus Callosum Body
Corpus Callosum Genu
Corpus Callosum Splenium
Left Cingulum
Right Cingulum
Left Corticospinal Tract
Right Corticospinal Tract
Left Fornix
Right Fornix
Left Inf. Frontal-Occipital Fasciculus
Right Inf. Frontal-Occipital Fasciculus
Left Inf. Longitudinal Fasciculus
Right Inf. Longitudinal Fasciculus
Left Sup. Longitudinal Fasciculus
Right Sup. Longitudinal Fasciculus
Left Uncinate Fasciculus
Right Uncinate Fasciculus
Global White Matter
C
3.00e-2
0
Rate of Change (ΔFDC/year)

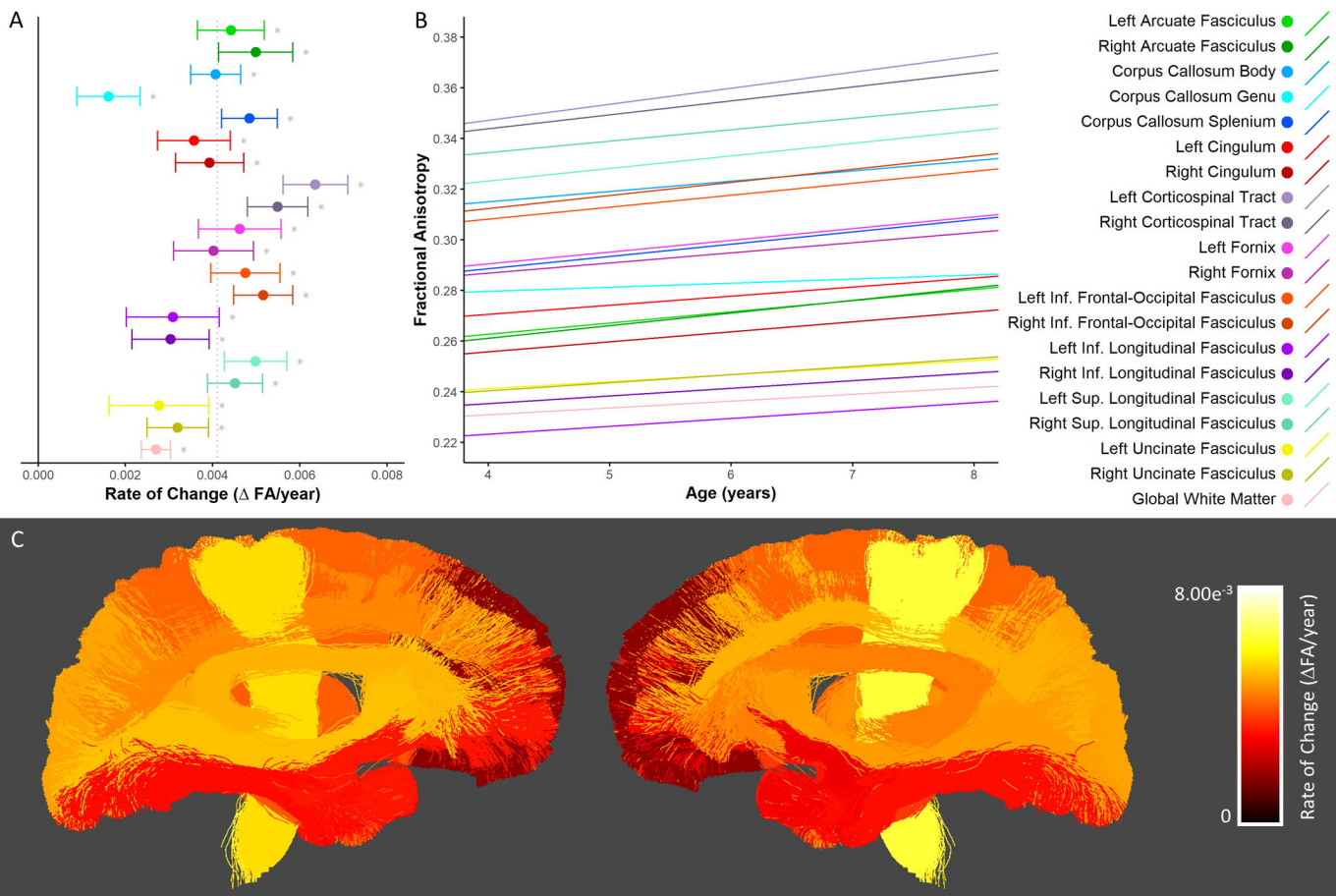
A
0.000
0.002
0.004
0.006
0.008
Rate of Change (Δ FA/year)
B
Fractional Anisotropy
0.38
0.36
0.34
0.32
0.30
0.28
0.26
0.24
0.22
4
5
6
7
8
Age (years)
Left Arcuate Fasciculus
Right Arcuate Fasciculus
Corpus Callosum Body
Corpus Callosum Genu
Corpus Callosum Splenium
Left Cingulum
Right Cingulum
Left Corticospinal Tract
Right Corticospinal Tract
Left Fornix
Right Fornix
Left Inf. Frontal-Occipital Fasciculus
Right Inf. Frontal-Occipital Fasciculus
Left Inf. Longitudinal Fasciculus
Right Inf. Longitudinal Fasciculus
Left Sup. Longitudinal Fasciculus
Right Sup. Longitudinal Fasciculus
Left Uncinate Fasciculus
Right Uncinate Fasciculus
Global White Matter
C
8.00e-3
0
Rate of Change (ΔFA/year)

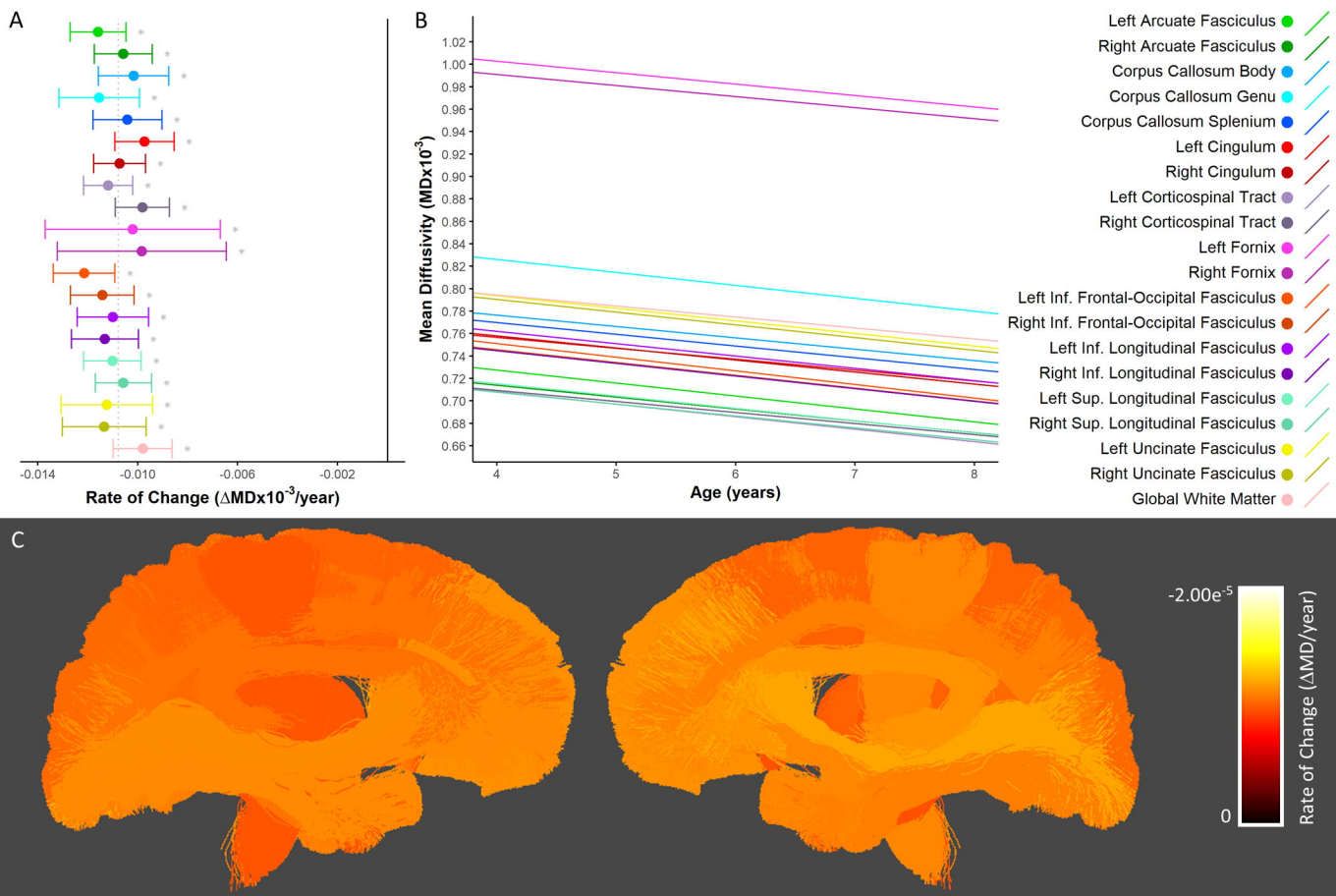
A
-0.014
-0.010
-0.006
-0.002
Rate of Change (ΔMDx10-3/year)
B
Mean Diffusivity (MDx10-3)
1.02
1.00
0.98
0.96
0.94
0.92
0.90
0.88
0.86
0.84
0.82
0.80
0.78
0.76
0.74
0.72
0.70
0.68
0.66
4
5
6
7
8
Age (years)
Left Arcuate Fasciculus
Right Arcuate Fasciculus
Corpus Callosum Body
Corpus Callosum Genu
Corpus Callosum Splenium
Left Cingulum
Right Cingulum
Left Corticospinal Tract
Right Corticospinal Tract
Left Fornix
Right Fornix
Left Inf. Frontal-Occipital Fasciculus
Right Inf. Frontal-Occipital Fasciculus
Left Inf. Longitudinal Fasciculus
Right Inf. Longitudinal Fasciculus
Left Sup. Longitudinal Fasciculus
Right Sup. Longitudinal Fasciculus
Left Uncinate Fasciculus
Right Uncinate Fasciculus
Global White Matter
C
-2.00e-5
0
Rate of Change (ΔMD/year)

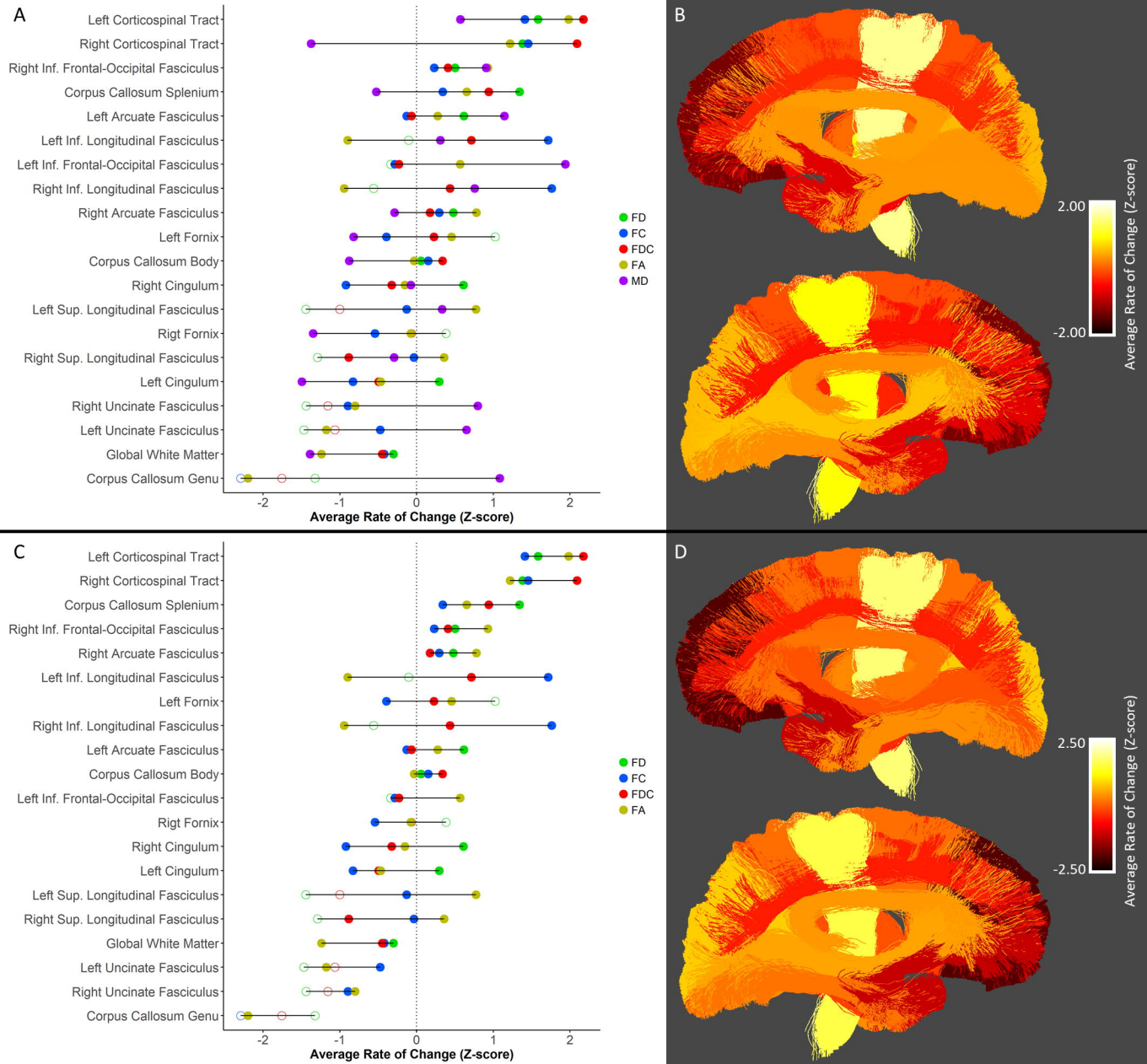
A
Left Corticospinal Tract
Right Corticospinal Tract
Right Inf. Frontal-Occipital Fasciculus
Corpus Callosum Splenium
Left Arcuate Fasciculus
Left Inf. Longitudinal Fasciculus
Left Inf. Frontal-Occipital Fasciculus
Right Inf. Longitudinal Fasciculus
Right Arcuate Fasciculus
Left Fornix
Corpus Callosum Body
Right Cingulum
Left Sup. Longitudinal Fasciculus
Rigt Fornix
Right Sup. Longitudinal Fasciculus
Left Cingulum
Right Uncinate Fasciculus
Left Uncinate Fasciculus
Global White Matter
Corpus Callosum Genu
-2
-1
0
1
2
Average Rate of Change (Z-score)
FD
FC
FDC
FA
MD
B
2.00
-2.00
Average Rate of Change (Z-score)
C
Left Corticospinal Tract
Right Corticospinal Tract
Corpus Callosum Splenium
Right Inf. Frontal-Occipital Fasciculus
Right Arcuate Fasciculus
Left Inf. Longitudinal Fasciculus
Left Fornix
Right Inf. Longitudinal Fasciculus
Left Arcuate Fasciculus
Corpus Callosum Body
Left Inf. Frontal-Occipital Fasciculus
Rigt Fornix
Right Cingulum
Left Cingulum
Left Sup. Longitudinal Fasciculus
Right Sup. Longitudinal Fasciculus
Global White Matter
Left Uncinate Fasciculus
Right Uncinate Fasciculus
Corpus Callosum Genu
-2
-1
0
1
2
Average Rate of Change (Z-score)
FD
FC
FDC
FA
D
2.50
-2.50
Average Rate of Change (Z-score)